

Stability of Grasping in a Static or Dynamic Sense

The first part of this chapter studies the geometry of grasping or immobilisation of a solid object by a number of frictionless fingers or fixtures. It shows that at least four frictionless contact points or four fixtures are required to immobilise planar objects. In particular, we show that three contact points are necessary and sufficient for immobilising a two-dimensional (2-D) triangular object but that four frictionless contacts or four fixtures are necessary and sufficient to immobilise a parallelepiped or to establish force/torque closure grasp. In the case of 3-D polyhedra, seven frictionless contact points are sufficient to establish a force/torque closure grasp.

The latter half of this chapter addresses another type of problem of grasping or immobilisation of a 2-D rigid object, in a dynamic sense: the simplest but most fundamental problem for stopping or immobilising rotational motion of a 2-D object with a flat side surface by a multi-joint robot finger where the object can only pivot around a single axis. It is assumed that rotational motion of the object pivoted around the fixed axis is frictionless and the finger-end is hemispherical and therefore rolling between the finger-end and object surfaces is induced without incurring any slip. Lagrange's equation of motion of such a testbed finger/object system is derived together with two constraints, the point contact constraint and the rolling contact constraint. It is shown that there arises a rolling constraint force tangential to both the finger-end sphere and the object surface originates at the contact point. Another simple testbed problem of dynamic grasping of a 2-D object by two one-DOF fingers with spherical ends is proposed, where motion of the overall system is confined to the horizontal plane. Rolling contacts play an essential role in stabilisation of dynamic grasping through force/torque balance. In the final section, a class of coordinated motor-control signals based on fingers-thumb opposition is shown to establish force/torque balance in a blind manner without knowing the object kinematics or using visual or tactile sensing.

2.1 Immobilisation of 2-D Objects

The problem of achieving a firm grip on an object is one of the most fundamental issues underlying the design and control of multi-fingered hands. There are two approaches for defining the motion of a firm grip; form closure and immobilisation. In this section, we deal with the problem of immobilising a planar polygonal object. In the case of three-dimensional polyhedral objects, we only show theoretical results without giving the proof.

Given a planar shape P in the horizontal plane, a set of points S is said to immobilise P if any rigid motion of P in the plane forces at least one point of S to penetrate the interior of P . By shape we mean a two-dimensional set of points bounded by a Jordan curve. Evidently, any minimal S contains only points belonging to the boundary of P . For the sake of gaining physical intuition into the problem, we treat only polygonal objects (therefore, the disc is excluded from this consideration).

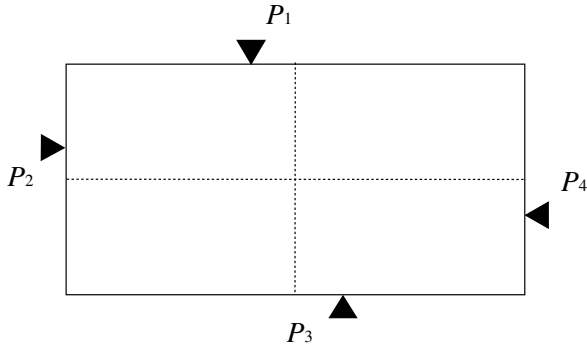
For example, consider the parallelepiped shown in Figure 2.1 and choose four points on the boundary as $S = \{P_1, P_2, P_3, P_4\}$. Apparently the set S immobilises this parallelepiped. However, if any one of points in S is excluded, then the set $S' = \{P_{i1}, P_{i2}, P_{i3}\}$ consisting of the remaining points does not immobilise the object. Indeed, for example, the set $S' = \{P_1, P_2, P_3\}$, any movement of P to the right does not make any point of S' penetrate the interior of P (that is, any fixed point P_i cannot get inside P by a certain infinitesimally small translational movement of P). Physically, a boundary point P_i of the set S for a shape P can be regarded as a contact with the boundary of P externally made by a rigid body, which is called a fixture (mainly, in the case of immobilisation) and a frictionless finger (in the case of form closure).

Next consider the problem of how many fixtures are necessary and sufficient to immobilise triangles. In general, four fixtures are enough to immobilise polygonal objects. We show the solution to the problem below.

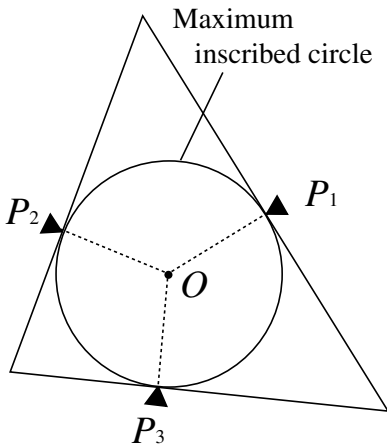
Theorem 2.1. Three fixtures are necessary and sufficient to immobilise any triangle.

To find a set of such contact points $S = \{P_1, P_2, P_3\}$ for the triangle P , let us consider the maximally inscribed circle of P [see Figure 2.1(b)] and choose $S = \{P_1, P_2, P_3\}$ by picking every point at which the inscribed circle touches the boundary of P . Intuitively this set $S = \{P_1, P_2, P_3\}$ seems to immobilise the triangle P . Nevertheless, the proof is not trivial.

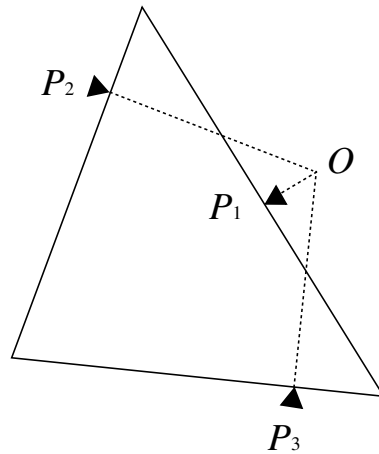
To confirm this, first observe that each contact point should lie on a different side of the triangle. Next, the three orthogonal lines to the boundary at the points P_1 , P_2 , and P_3 should meet at a common point. To show this, suppose that the three orthogonal lines do not meet at a single point. Then, these three orthogonals constitute a triangle as shown in Figure 2.2, where we denote the original triangle by its vertices $\{A, B, C\}$. Let O be a point in the interior of the triangle constituted by the three orthogonals. Then, the three angles $\angle OP_1B$, $\angle OP_2C$ and $\angle OP_3A$ are all acute, as shown in Figure 2.2.



(a) Immobilisation of a parallelepiped



(b) Immobilisation of a triangle



(c) Immobilisation of a triangle

Fig. 2.1. Three fixtures are necessary and sufficient to immobilise triangles. In general, four fixtures are enough to immobilise polygonal objects.

Or, for some choices for $S = \{P_1, P_2, P_3\}$, all three of these angles become obtuse. Therefore, in the case shown in Figure 2.2, the triangle $\{A, B, C\}$ can be rotated counterclockwise by a small angle around O and the points $\{P_1, P_2, P_3\}$ remain outside the interior of $\{A, B, C\}$. In the latter case, the triangle $\{A, B, C\}$ can be rotated clockwise by a small angle. In either case, the existence of such a rotation around O contradicts immobilisation of the triangle. It is also possible to prove that the concurrency of the three orthogonals at the contact points $\{P_1, P_2, P_3\}$ is also a sufficient condition for immobilisation of the triangle. However, we omit the proof of this sufficiency but state this main result in the following theorem.

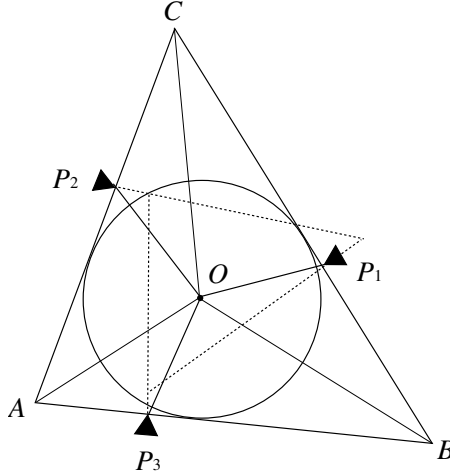


Fig. 2.2. The set $S = \{P_1, P_2, P_3\}$ cannot immobilise this triangle

Theorem 2.2. A necessary and sufficient condition for immobilising a triangle $\{A, B, C\}$ by the contact points $S = \{P_1, P_2, P_3\}$ is that the three orthogonals at P_i ($i = 1, 2, 3$) to the corresponding sides meet at a common single point.

Finally, we mention the following two results without proof.

Theorem 2.3. Any polygonal object in the plane can always be immobilised by using four fixtures (contact points).

Theorem 2.4. Any polygonal object containing no parallel sides can be immobilised by finding three fixtures.

Further, we summarize the theoretical results about immobilisation of polyhedra obtained and proved in the literature in the following two theorems.

Theorem 2.5. Any three-dimensional polyhedron can be immobilised by using six fixtures.

Theorem 2.6. Any n -dimensional polytope can be immobilised by using $2n$ fixtures.

2.2 Force/Torque Closure

Another concept of a firm grip on a rigid object is form closure (equivalently called force/torque closure), which is a finite set of wrench vectors (force-moment combinations) applied on the object with the property that any other wrench vector acting on the object can be balanced by a positive combination

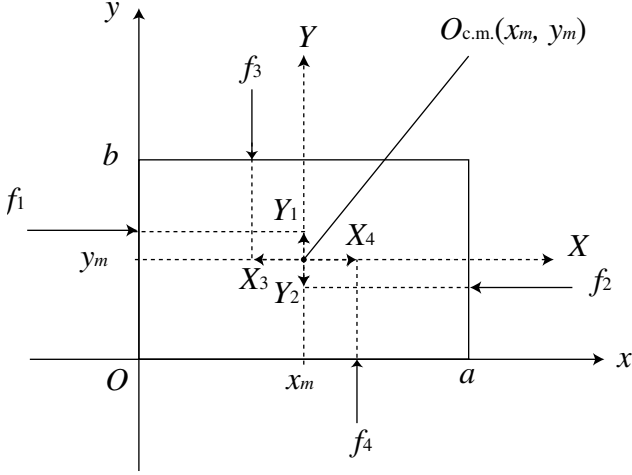


Fig. 2.3. The set of four forces $\{f_1, f_2, f_3, f_4\}$ directed normally to the four sides of the parallelepiped, respectively, achieves force/torque closure

of the original ones. It has already been pointed out that the form closure of a two-dimensional object requires at least four wrench vectors and that of a three-dimensional object requires at least seven wrench vectors. It is also known that these numbers can be achieved by wrench vectors realisable as forces normal to the surface of the object. Such wrench vectors are equivalent to the supposition of frictionless fingers contacting pointwise to the object surface. To gain physical insight into the concept of form closure, we discuss first a problem of firm grip of a parallelepiped as an illustrative example of two-dimensional objects.

Consider now a rigid parallelepiped lying on a horizontal xy -plane with four sides as shown in Figure 2.3, and suppose that four forces \mathbf{f}_i ($i = 1, 2, 3, 4$) are acting on different sides as in the figure. If we denote the magnitude of the force vector \mathbf{f}_i by the positive number f_i and set the coordinates (x, y) as shown in Figure 2.3, the forces \mathbf{f}_i ($i = 1, \dots, 4$) can be expressed by the vectors $\mathbf{f}_1 = (f_1, 0)^T$, $\mathbf{f}_2 = (-f_2, 0)^T$, $\mathbf{f}_3 = (0, -f_3)^T$ and $\mathbf{f}_4 = (0, f_4)^T$. When the force \mathbf{f}_1 is exerted on the object, the rotational moment with a magnitude $|f_1 Y_1|$ arises clockwise around the object mass centre $O_{c.m.}$ as shown in Figure 2.3. In the figure, all variables Y_i ($i = 1, 2$) and X_i ($i = 3, 4$) are defined. If we append such a rotational moment $f_i Y_i$ ($i = 1, 2$) or $f_i X_i$ ($i = 3, 4$) to \mathbf{f}_i by letting the sign of a counter-clockwise moment be positive, then it is possible to consider the following four three-dimensional vectors:

$$\mathbf{w}_1 = \begin{pmatrix} f_1 \\ 0 \\ -f_1 Y_1 \end{pmatrix}, \quad \mathbf{w}_2 = \begin{pmatrix} -f_2 \\ 0 \\ f_2 Y_2 \end{pmatrix}, \quad \mathbf{w}_3 = \begin{pmatrix} 0 \\ -f_3 \\ -f_3 X_3 \end{pmatrix}, \quad \mathbf{w}_4 = \begin{pmatrix} 0 \\ f_4 \\ f_4 X_4 \end{pmatrix}. \quad (2.1)$$

Such a vector \mathbf{w}_i is called a two-dimensional wrench vector. In the three-dimensional case, such a wrench vector is expressed by the six-dimensional vector $\mathbf{w} = (\mathbf{f}, \mathbf{r} \times \mathbf{f})^T$, where \mathbf{f} stands for the three-dimensional force vector acting at a contact point normally to the object boundary surface and \mathbf{r} is the position vector originating from the object mass centre and terminating at the contact point. The symbol \times means the vector outer product.

Definition 2.1. Suppose that n frictionless fingers are applied to a rigid object at different points with n wrench vectors $W = \{\mathbf{w}_1, \dots, \mathbf{w}_n\}$. If any external wrench \mathbf{w}_{ex} applied to the object can be balanced by pressing fingertips against the object at the selected contact points, the grasp with the set W of wrench vectors is said to be form-closure (or force/torque closure).

In more detail, the grasp W is form-closure if and only if for any external wrench \mathbf{w}_{ex} it is possible to find a set of non-negative parameters $\alpha_i \geq 0$ ($i = 1, \dots, n$) that satisfy

$$\sum_{i=1}^n \alpha_i \mathbf{w}_i + \mathbf{w}_{\text{ex}} = 0. \quad (2.2)$$

This formula expresses the fact that external wrench \mathbf{w}_{ex} can be balanced by the set of original fingers through modifying the magnitudes of the forces f_i to $\alpha_i f_i$ ($i = 1, \dots, n$).

For example, in the case of the 2-D object shown in Figure 2.3, the set W of four wrench vectors given in Equation (2.1) achieves force/torque closure if f_i ($i = 1, \dots, 4$) satisfies

$$f_1 = f_2 > 0, \quad f_3 = f_4 > 0, \quad f_1 Y_1 = f_3 X_3 \quad (2.3)$$

provided that

$$Y_1 + Y_2 = 0, \quad X_3 + X_4 = 0. \quad (2.4)$$

This can be explicitly confirmed by the following argument.

For a given set of wrench vectors $W = \{\mathbf{w}_1, \dots, \mathbf{w}_n\}$, let us consider the normalised set of wrenches $\bar{W} = \{\bar{\mathbf{w}}_1, \dots, \bar{\mathbf{w}}_n\}$, where $\bar{\mathbf{w}}_i = \mathbf{w}_i / \|\mathbf{w}_i\|$, $i = 1, \dots, n$, and $\|\mathbf{w}\|$ denotes the Euclidean norm of vectors \mathbf{w} . Then, consider a set of all points P such that

$$P = \sum_{i=1}^n \gamma_i \mathbf{w}_i, \quad \sum_{i=1}^n \gamma_i = 1, \quad \gamma_i \geq 0 \quad (i = 1, \dots, n) \quad (2.5)$$

and denote the set by $H(W)$, and call it the convex hull of the set of original wrench vectors W .

Theorem 2.7. A necessary and sufficient condition for a grasp with a set of wrench vectors W to reach form-closure is that the origin of the wrench space lies exactly inside the convex hull $H(W)$ of the original set W of wrench vectors.

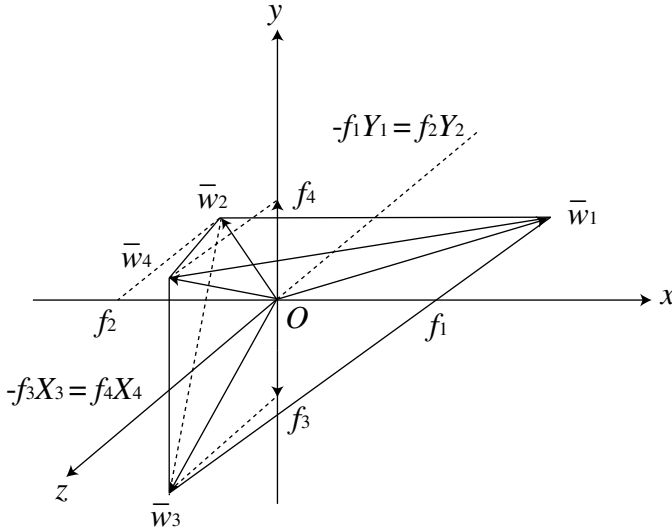


Fig. 2.4. The convex hull $H(\bar{W})$ composed of four normalised wrenches $\bar{W} = \{\bar{w}_1, \bar{w}_2, \bar{w}_3, \bar{w}_4\}$ includes the origin O as an interior point

In the case of the parallelepiped shown in Figure 2.3 with wrench vectors $W = \{w_1, w_2, w_3, w_4\}$ satisfying Equations (2.3) and (2.4), the convex hull of W can easily be constructed as shown in Figure 2.4, from which it is possible to see that the origin O is exactly inside $H(W)$. This shows that the grasp with this W achieves force/torque closure.

Straightforwardly from Theorem 2.2, it follows that

Theorem 2.8. The form closure of a two-dimensional object requires at least four wrenches and that of a three-dimensional object requires at least seven wrenches.

Theorem 2.9. Form closure of any two-dimensional bounded object (except a circle) can be achieved by four frictionless fingers. For three dimensions, form closure of three-dimensional objects with rotational symmetries can be achieved with seven frictionless fingers.

It is also shown that

Theorem 2.10. For any convex polygon, four contact points $S = \{P_1, \dots, P_4\}$ at which the set of wrenches achieves form closure can immobilise a polygonal object.

It is interesting to note that any three wrench vectors constructed at three contact points $S = \{P_1, P_2, P_3\}$ of a triangle shown in Figure 2.1(b) cannot achieve form closure, even if the three orthogonals meet at a common point (that is, S immobilises the triangle).

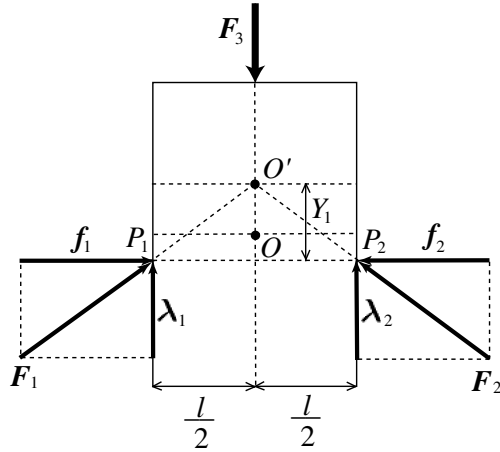


Fig. 2.5. Frictional fingers press the object against the sides in the directions of \mathbf{F}_1 and \mathbf{F}_2 due to the existence of the frictional forces λ_1 and λ_2 tangent to the object surface

2.3 Frictional Grasp of 2-D Objects

In our everyday life, we pick up small objects on a desk quite easily by using a thumb and index finger without dropping them. As a matter of course, our thumb and fingers are not rigid but soft and flexible. In fact, our finger-end has a curved surface and makes contact with a rigid object with some contacted area caused by deformation of the finger-end soft material. Then, there may arise a frictional force in the direction tangent to the contact area due to both static and viscous (dynamic) friction. Even if the finger-end is rigid but has a curved surface, it may cause rolling on the object surface without sliding or slipping. In the next section, we will show that such rolling constraint induces a constraint force in the direction tangential to both the finger-end and object surfaces. This tangential force is a constraint force and hence is irrelevant to energy consumption during motion, unlike the viscous friction.

In this section, we treat a force/torque closure problem for a 2-D rectangular object by using a pair of frictional fingers. Two frictional forces \mathbf{F}_1 and \mathbf{F}_2 acting at points P_1 and P_2 , respectively, against the object can be regarded as a sum of components \mathbf{f}_i normal and λ_i tangent to the object side ($i = 1, 2$), as shown in Figure 2.5. Suppose that two straight lines drawn from P_1 and P_2 in the directions of \mathbf{F}_1 and \mathbf{F}_2 , respectively, meet at a point O' . In other words, assume that the direction of \mathbf{f}_2 is just opposite to that of \mathbf{f}_1 and the straight line including the line segment $\overline{OO'}$ (where O denotes the centre of the rectangular) splits the rectangular into two parts with the same shape and size. If we regard the point O' as the origin of (x, y) -coordinates as in Figure 2.3, then the vectors \mathbf{f}_i and λ_i ($i = 1, 2$) can be expressed in the

following way:

$$\mathbf{f}_1 = f_1 \begin{pmatrix} 1 \\ 0 \end{pmatrix}, \quad \mathbf{f}_2 = f_2 \begin{pmatrix} -1 \\ 0 \end{pmatrix}, \quad \lambda_1 = \lambda_1 \begin{pmatrix} 0 \\ -1 \end{pmatrix}, \quad \lambda_2 = \lambda_2 \begin{pmatrix} 0 \\ -1 \end{pmatrix}, \quad (2.6)$$

where all the f_i and λ_i ($i = 1, 2$) are positive constants. Correspondingly to these four force vectors, the wrench vectors are given as follows:

$$\begin{aligned} \mathbf{w}_{f1} &= f_1 \begin{pmatrix} 1 \\ 0 \\ Y_1 \end{pmatrix}, \quad \mathbf{w}_{f2} = f_2 \begin{pmatrix} -1 \\ 0 \\ -Y_1 \end{pmatrix}, \\ \mathbf{w}_{\lambda1} &= \lambda_1 \begin{pmatrix} 0 \\ -1 \\ -l/2 \end{pmatrix}, \quad \mathbf{w}_{\lambda2} = \lambda_2 \begin{pmatrix} 0 \\ -1 \\ l/2 \end{pmatrix}. \end{aligned} \quad (2.7)$$

Evidently, the set of wrenches $W = \{\mathbf{w}_{f1}, \mathbf{w}_{f2}, \mathbf{w}_{\lambda1}, \mathbf{w}_{\lambda2}\}$ does not realise force/torque closure, because the sum of these four wrenches cannot be balanced except for the case $f_1 = f_2 = 0$ and $\lambda_1 = \lambda_2 = 0$. That is, the origin cannot be included inside $H(W)$, the convex hull of W . Then, let us consider the situation that the external force \mathbf{F}_3 is exerted on the rectangular object in the direction of the y -axis, down from the top, as shown in Figure 2.5. If this 2-D object with mass M is placed in a vertical plane and subjected to gravity, this external force \mathbf{F}_3 can be regarded as the gravity force expressed by $\mathbf{F}_3 = Mg(0, 1)^T$. Then it is easy to see that the set of wrenches W and this additional wrench $\mathbf{w}_{F3} = Mg(0, 1, 0)^T$ can be balanced by setting

$$f_1 = f_2 > 0, \quad \lambda_1 = \lambda_2 = Mg/2, \quad (2.8)$$

which yields

$$\sum_{i=1,2} (\mathbf{w}_{fi} + \mathbf{w}_{\lambda i}) + \mathbf{w}_{F3} = 0. \quad (2.9)$$

It is interesting to note that the set of five wrenches $W' = \{\mathbf{w}_{f1}, \mathbf{w}_{f2}, \mathbf{w}_{\lambda1}, \mathbf{w}_{\lambda2}, \mathbf{w}_{F3}\}$ achieves force/torque closure, because the convex hull $H(W')$ apparently includes the origin as an interior point. In fact, suppose that a small external force with wrench $\mathbf{w}_d = (\varepsilon_x, \varepsilon_y, \varepsilon_m)^T$ is exerted on the rectangular object. In order to balance \mathbf{w}_d by the set W' , it is necessary and sufficient to choose $f_i > 0$ and $\lambda_i > 0$ while fixing the value Mg so that

$$\sum_{i=1,2} (\mathbf{w}_{fi} + \mathbf{w}_{\lambda i}) + \mathbf{w}_{F3} + \mathbf{w}_d = 0. \quad (2.10)$$

This equality can be satisfied by choosing $f_i > 0$ and $\lambda_i > 0$ so that they satisfy

$$\begin{cases} f_1 - f_2 = -\varepsilon_x, & \lambda_1 + \lambda_2 = Mg + \varepsilon_y \\ -\varepsilon_x Y_1 - l\lambda_1 + \frac{l}{2}(Mg + \varepsilon_y) + \varepsilon_m = 0 \end{cases} \quad (2.11)$$

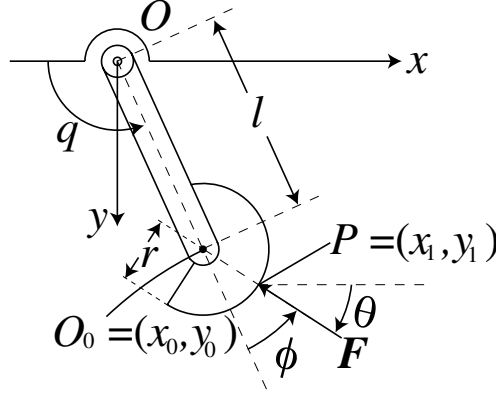


Fig. 2.6. A single-joint finger robot receives an external force \mathbf{F} in the direction from P to O_0

from which it follows that

$$\begin{cases} f_i = f_d + (-1)^i \frac{\varepsilon_x}{2} \\ \lambda_i = \frac{1}{2}(Mg + \varepsilon_y) + (-1)^i \frac{\varepsilon_x Y_1 - \varepsilon_m}{l} \end{cases} \quad i = 1, 2. \quad (2.12)$$

where f_d is a certain appropriate positive constant. Conversely, it is easy to check that if f_i and λ_i are chosen by Equation (2.12) then the force/torque balance expressed by Equation (2.10) is realized. The arguments imply a potential way of controlling the grasp of a 2-D polygonal object by using a pair of fingers that exert not only pressing forces on the object normal to the object surface but also frictional (or rolling constraint) forces tangent to it.

2.4 Rolling Contact Constraint

Before discussing how rolling constraint force emerges from the physical interaction of rolling between a robot finger-end and a 2-D object surface and how effectively it is used to balance the force/torque, we show how an external force acting on a robot finger enters Lagrange's equation of motion for the finger. First, consider the single DOF finger depicted in Figure 2.6 on which the external force \mathbf{F} is exerted at a fixed point P at a distance from the centre of curvature O_0 of the spherical finger-end r . The finger is composed of a rigid link with length l whose end is rigidly connected to the finger-end and therefore the link together with the finger-end is regarded as a single rigid body. Denote the pivoted origin of the robot finger by O and set the (x, y) coordinates as shown in Figure 2.6. Then, the positions O_0 and P can be expressed as

$$\begin{cases} O_0 = \begin{pmatrix} x_0 \\ y_0 \end{pmatrix} = \begin{pmatrix} -l \cos q \\ l \sin q \end{pmatrix} \\ P = \begin{pmatrix} x_1 \\ y_1 \end{pmatrix} = \begin{pmatrix} -l \cos q - r \cos(q + \phi) \\ l \sin q + r \sin(q + \phi) \end{pmatrix} \end{cases} \quad (2.13)$$

where the angles q and ϕ are defined in Figure 2.6. Since in this case the xy -plane is regarded as horizontal, the effect of gravity can be ignored. At the same time, we assume that rotational motion of the robot finger is frictionless. Evidently, the kinetic energy of the robot finger is denoted by $K = (1/2)I\dot{q}^2$ and the external force is expressed as

$$\mathbf{F} = F (\cos(q + \phi), -\sin(q + \phi))^T, \quad (2.14)$$

where I denotes the moment of inertia of the finger around O and F denotes the magnitude of \mathbf{F} . Then, applying the variational principle to the Lagrangian $L = K$ with the external force \mathbf{F} yields

$$\int_{t_0}^{t_1} \left\{ \delta L + \frac{\partial(x_1, y_1)}{\partial q} \mathbf{F} \delta q \right\} dt = 0 \quad (2.15)$$

from which it follows that

$$I\ddot{q} = J^T(q)\mathbf{F}, \quad (2.16)$$

where

$$J(q) = \begin{pmatrix} \partial x_1 / \partial q \\ \partial y_1 / \partial q \end{pmatrix} = \begin{pmatrix} l \sin q + r \sin(q + \phi) \\ l \cos q + r \cos(q + \phi) \end{pmatrix}. \quad (2.17)$$

Hence, the right-hand side of Equation (2.15) can be calculated by using the expressions for \mathbf{F} and $J(q)$ [Equations (2.13) and (2.16)] in such a way that

$$\begin{aligned} J^T(q)\mathbf{F} &= -lF \{ \sin q \cos(q + \phi) - \cos q \sin(q + \phi) \} \\ &\quad - rF \{ \sin(q + \phi) \cos(q + \phi) - \cos(q + \phi) \sin(q + \phi) \} \\ &= -LF \sin \phi. \end{aligned} \quad (2.18)$$

Thus, Equation (2.15) can be written in the form

$$I\ddot{q} = -lF \sin \phi. \quad (2.19)$$

This shows that the external force \mathbf{F} acting at the finger-end surface in the direction normal to it can be regarded as being acting at the centre of curvature of the finger-end sphere in the same direction. Furthermore, suppose that an appropriate servo-motor actuator is installed at the pivotal joint O to generate control torque signals, and denote the control input torque by u . Then, this control torque can be regarded as an external torque at joint O

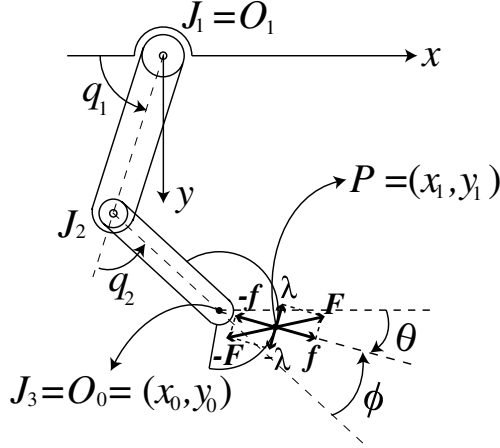


Fig. 2.7. A two-DOF finger robot receives an external force $-\mathbf{F}$ that can be regarded as the sum of component forces $-\mathbf{f}$ and $-\boldsymbol{\lambda}$ orthogonal to each other

and hence it is possible to express the equation of motion of the robot finger in the following form:

$$I\ddot{q} = -lF \sin \phi + u. \quad (2.20)$$

If all physical parameters l , F and ϕ are known, it is possible to design a control input u to stop the rotational motion of the finger by setting $u = lF \sin \phi$ so as to withstand and balance the external force \mathbf{F} .

Next consider the case of a two-DOF finger robot with a spherical end with an external force $-\mathbf{F}$ exerted at the point $P (= (x_1, y_1))$ as shown in Figure 2.7. For the convenience of discussions in subsequent sections, in this case we use a minus sign to express the external force. This external force can be regarded as the sum of two components $-\mathbf{f}$ and $-\boldsymbol{\lambda}$ as shown in Figure 2.7. Here the direction of $-\mathbf{f}$ is normal to the finger-end surface and that of $-\boldsymbol{\lambda}$ is tangential to it. In order to derive Lagrange's equation of motion, denote the kinetic energy of the finger robot with two joints by

$$K = K(q, \dot{q}) = \frac{1}{2} \dot{q}^T(t) H(q(t)) \dot{q}(t) \quad (2.21)$$

where $q = (q_1, q_2)^T$ and $H(q)$ denotes the inertia matrix of the planar robot finger with two DOFs as expressed in Equation (1.107). Then, the variational principle in this case can be described by the following form:

$$\int_{t_0}^{t_1} \left[\delta K + \left\{ \frac{\partial(x_0, y_0)}{\partial q} \mathbf{f} + \frac{\partial(x_1, y_1)}{\partial q} \boldsymbol{\lambda} + u^T \delta q \right\} \right] dt = 0. \quad (2.22)$$

where $u = (u_1, u_2)^T$ denotes the control torques generated at joint actuators. Note that $-\mathbf{f}$ and $-\boldsymbol{\lambda}$ can be described as

$$\begin{cases} -\mathbf{f} = f \begin{pmatrix} \cos(q_1 + q_2 + \phi) \\ -\sin(q_1 + q_2 + \phi) \end{pmatrix} = -f \begin{pmatrix} \cos \theta \\ -\sin \theta \end{pmatrix}, \\ -\lambda = -\lambda \begin{pmatrix} \sin(q_1 + q_2 + \phi) \\ \cos(q_1 + q_2 + \phi) \end{pmatrix} = \lambda \begin{pmatrix} \sin \theta \\ \cos \theta \end{pmatrix}, \end{cases} \quad (2.23)$$

where θ denotes the angle from the x -axis to the direction of the external force \mathbf{f} . Since the sign of the angle in a counter-clockwise direction is taken to be positive, the angle θ in the case of Figure 2.7 is negative. Furthermore, it is possible to write the position P relative to the position O_0 in the following way:

$$\begin{pmatrix} x_1 \\ y_1 \end{pmatrix} = \begin{pmatrix} x_0 + r \cos(q_1 + q_2 + \phi) \\ y_0 - r \sin(q_1 + q_2 + \phi) \end{pmatrix} = \begin{pmatrix} x_0 \\ y_0 \end{pmatrix} + r \begin{pmatrix} \cos \theta \\ -\sin \theta \end{pmatrix}. \quad (2.24)$$

Further, it follows that

$$\frac{\partial(x_1, y_1)}{\partial q} = J_0^T(q) - r \begin{pmatrix} \sin \theta & \cos \theta \\ \sin \theta & \cos \theta \end{pmatrix}, \quad (2.25)$$

where

$$J_0^T(q) = \frac{\partial(x_0, y_0)}{\partial q}. \quad (2.26)$$

Hence, from Equations (2.23) and (2.25) it follows that

$$-\frac{\partial(x_1, y_1)}{\partial q} \mathbf{f} = -f J_0^T(q) \begin{pmatrix} \cos \theta \\ -\sin \theta \end{pmatrix}, \quad (2.27)$$

$$-\frac{\partial(x_1, y_1)}{\partial q} \lambda = \lambda \left\{ J_0^T(q) \begin{pmatrix} \sin \theta \\ \cos \theta \end{pmatrix} - r \begin{pmatrix} 1 \\ 1 \end{pmatrix} \right\}. \quad (2.28)$$

Thus, it follows from the variational principle expressed as Equation (1.85) that

$$\begin{aligned} H(q)\ddot{q} + \left\{ \frac{1}{2}\dot{H}(q) + S(q, \dot{q}) \right\} + f J_0^T(q) \begin{pmatrix} \cos \theta \\ -\sin \theta \end{pmatrix} \\ - \lambda \left\{ J_0^T(q) \begin{pmatrix} \sin \theta \\ \cos \theta \end{pmatrix} - r \begin{pmatrix} 1 \\ 1 \end{pmatrix} \right\} = u. \end{aligned} \quad (2.29)$$

It is important to note that, for the generation of two torque components to counter-balance the torques exerted by the external force $-\mathbf{F}$ whose direction is changing instantaneously (ϕ is not constant), two independent actuators installed separately at two joints are necessary. In other words, if u is a scalar control variable and hence $J_0^T(q)$ is a 1×2 matrix, the total sum of the third and fourth terms of the left-hand side of Equation (2.29) cannot be restored into such two original terms.

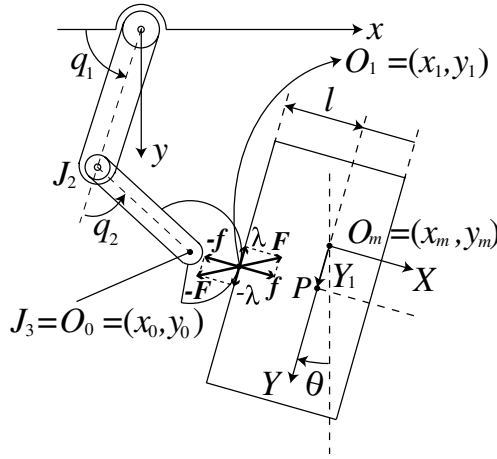


Fig. 2.8. A two-DOF finger robot immobilising a 2-D object pivoted at a fixed point

2.5 Testbed Problems for Dynamically Stable Grasp

For the study of stable grasping and dexterous manipulation by a human-like multi-fingered hand, a simple but canonical testbed problem underlying control of motion of the simplest robot mechanism is very useful for gaining both physical and mathematical insights into the problem. Such a prototype problem may play a similar role to the well-known problem of stability and control of the inverted pendulum that has contributed to advances in linear and non-linear control theory of mechanical systems. However, there is a noteworthy difference between the two testbed problems. Even in the case of the simpler testbed problems of stable grasp, Lagrange's equation of motion for a robot mechanism is subject to geometric constraints and therefore control inputs cannot enter explicitly into the equation of motion of the object to be controlled. Grasping an object should be controlled indirectly through constraint forces.

For the sake of mechanical simplicity but still to show the key role of the rolling constraint, let us consider the mechanical setup shown in Figure 2.8, which is composed of a two-DOF robot finger with a hemispherical finger-end and a rigid rectangular 2-D object pinned at a point O_m but pivoting around it. It is assumed that the xy -plane is horizontal and the whole motion of the finger and object is confined to this plane and therefore the effect of gravity can be ignored. For convenience and simplicity, we assume further that rotational motion of the object around the O_m is frictionless. Comparing Figure 2.8 with Figure 2.7, we can easily see that the equation of rotational motion of the object follows directly from Newton's law of action and reaction in the following form:

$$I\ddot{\theta} - fY_1 + \lambda l = 0, \quad (2.30)$$

where I denotes the inertia moment of the object around O_m , l the distance from O_m to the left rectilinear side of the object as shown in Figure 2.8 and Y_1 the Y -component of the (X, Y) -coordinates of position O_1 attached at the object. The equation of motion of the finger is the same as that described by Equation (2.29) in the previous section. These two equations are derived, however, by assuming that there arises a force \mathbf{F} pressing the object in the direction shown in Figure 2.8 and a reactive force $-\mathbf{F}$ affecting the finger at the common point O_1 in the opposite direction.

We now show that these active and reactive forces \mathbf{F} and $-\mathbf{F}$, which have tangential components $\boldsymbol{\lambda}$ and $-\boldsymbol{\lambda}$, actually arise at the contact point O_1 between the finger-end and the object surface. In reality, the physical situation of contacting of the finger-end with the object should be expressed firstly by the algebraic equation

$$r + l = (x_m - x_0) \cos \theta + (y_m - y_0) \sin \theta. \quad (2.31)$$

Since the length of the line from O_0 to P (see Figure 2.8) is $r + l$ it must also be equal to the right-hand side of Equation (2.31). Here, P is a point at which the extended straight line from O_0 to O_1 crosses the Y -axis originates from the origin O_m . Secondly, if the spherical finger-end is rolling on the object surface without slipping then the contact point velocity expressed on the finger-end must be equal to that expressed on the object surface. This can be written as

$$\frac{d}{dt}(r\phi) = -\frac{d}{dt}Y_1, \quad (2.32)$$

where ϕ denotes the angle specified in Figure 2.7. It is easy to verify that

$$\phi = \pi + \theta - q_1 - q_2 = \pi + \theta - q^T \mathbf{e}, \quad (2.33)$$

$$Y_1 = (x_0 - x_m) \sin \theta + (y_0 - y_m) \cos \theta, \quad (2.34)$$

where $\mathbf{e} = (1, 1)^T$ and $q = (q_1, q_2)^T$. Note that Equation (2.32) can be integrated as follows:

$$r\phi(t) = -Y_1(t) - c_0, \quad (2.35)$$

where c_0 denotes a constant of integration. Thus, it follows from Equation (2.31) and substituting Equations (2.33) and (2.34) into Equation (2.35) that

$$\begin{aligned} Q(q, \theta) &= -(r + l) + (x_m - x_0) \cos \theta - (y_m - y_0) \sin \theta \\ &= 0, \end{aligned} \quad (2.36)$$

$$\begin{aligned} R(q, \theta) &= c_0 + Y + r\phi \\ &= c_0 + (x_0 - x_m) \sin \theta + (y_0 - y_m) \cos \theta + r(\pi + \theta - q^T \mathbf{e}) \\ &= 0. \end{aligned} \quad (2.37)$$

We call Equation (2.36) the contact constraint and Equation (2.37) the rolling constraint. Both constraints can be regarded as holonomic. Then, by introducing Lagrange's multipliers f and λ for Equations (2.36) and (2.37), respectively, we can define the Lagrangian

$$L = K + fQ + \lambda R, \quad (2.38)$$

where K denotes the kinetic energy expressed by Equation (2.21). Applying the variational principle described by Equation (1.76) to this Lagrangian, we obtain the following Lagrange's equation of motion:

$$H(q)\ddot{q} + \left\{ \frac{1}{2}\dot{H}(q) + S(q, \dot{q}) \right\} \dot{q} - f \frac{\partial Q}{\partial q} - \lambda \frac{\partial R}{\partial q} = u, \quad (2.39)$$

$$I\ddot{\theta} - f \frac{\partial Q}{\partial \theta} - \lambda \frac{\partial R}{\partial \theta} = 0. \quad (2.40)$$

Obviously, Equation (2.39) expresses the motion of the robot finger and Equation (2.40) the rotational motion of the object. The gradient vectors $\partial Q/\partial q$ and $\partial R/\partial q$ and partial differentials of Q and R with respect to θ can be calculated as follows:

$$\begin{cases} \frac{\partial Q}{\partial q} = -\frac{\partial(x_0, y_0)}{\partial q} \begin{pmatrix} \cos \theta \\ -\sin \theta \end{pmatrix} = -J_0^T(q) \begin{pmatrix} \cos \theta \\ -\sin \theta \end{pmatrix}, \\ \frac{\partial R}{\partial q} = \frac{\partial(x_0, y_0)}{\partial q} \begin{pmatrix} \sin \theta \\ \cos \theta \end{pmatrix} - r\mathbf{e} = J_0^T(q) \begin{pmatrix} \sin \theta \\ \cos \theta \end{pmatrix} - r\mathbf{e}, \\ \frac{\partial Q}{\partial \theta} = Y_1, \quad \frac{\partial R}{\partial \theta} = -l. \end{cases} \quad (2.41)$$

Thus, it is possible to confirm that substituting these partial differentials from Equation (2.41) into Equations (2.39) and (2.40) yields Equations (2.29) and (2.30). Evidently the Lagrange multiplier f acts at the contact point as a pressing force against the object and induces the rotational moment $-fY_1$ for the object around O_m . Similarly, another multiplier λ induces the rotational moment λl for the object around Q_m . Then, their two-dimensional wrenches acting on the object are written as follows:

$$\mathbf{w}_f = f \begin{pmatrix} \cos \theta \\ -\sin \theta \\ Y_1 \end{pmatrix}, \quad \mathbf{w}_\lambda = \lambda \begin{pmatrix} -\sin \theta \\ -\cos \theta \\ -l \end{pmatrix}. \quad (2.42)$$

Apparently, \mathbf{w}_f acts at the contact point as a pressing force for the object in the direction normal to the object side and \mathbf{w}_λ acts at the same contact point as a shear force along the object side. The typical testbed control problem for the set of motion Equations (2.29) and (2.30) that are subject to the constraint

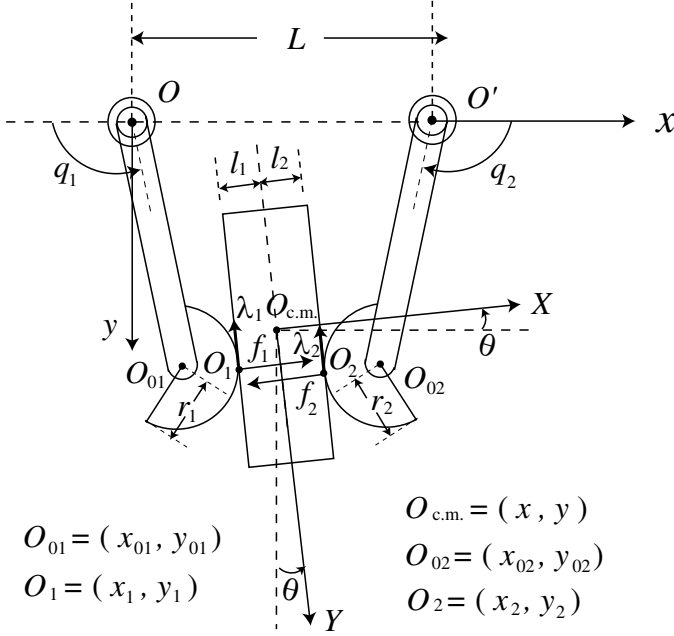


Fig. 2.9. A pair of single-DOF robot fingers grasping a 2-D rigid object with parallel surfaces

Equations (2.36) and (2.37) is to design a controller for stabilising rotational motion of the object by balancing induced moments of the object around O_m and maintaining some still state with a constant angle of θ and zero angular velocity $\dot{\theta} = 0$. Note that the control variables $u = (u_1, u_2)^T$ do not enter into the dynamics of the object, *i.e.*, Equation (2.30). The motion of the object should be indirectly controlled and stabilised through the constraint forces f and λ . This problem will be investigated in detail in subsequent sections, which will help us in understanding physical meanings of control of precision prehension by a pair of human-like robot fingers.

Next we shall propose another testbed problem of stable grasp with a simple mechanical structure. Let us consider a pair of single-DOF robot fingers whose ends are spherical and a 2-D object which has parallel sides, as shown in Figure 2.9. The motion of the overall fingers-object is confined to the horizontal xy -plane. In this case, it is implicitly assumed that an object with a flat bottom is placed on a desk and both the translational and rotational motions of the object are frictionless. In contrast to the previous example of Figure 2.8, the centre of mass $O_{c.m.}$ of the object is free to move. Denote the mass and the inertia moment of the object around $O_{c.m.}$ by M and I , respectively. All other physical variables are specified in Figure 2.9, as in Figures 2.7 and 2.8 except that in Figure 2.9 the position of the object centre of mass

is expressed by the vector $\mathbf{x} = (x, y)^T$ in terms of the frame coordinates with origin O . Hence, the total kinetic energy of this overall fingers-object system is expressed as

$$K = \sum_{i=1,2} \frac{1}{2} I_i \dot{q}_i^2 + \frac{M}{2} (\dot{x}^2 + \dot{y}^2) + \frac{I}{2} \dot{\theta}^2, \quad (2.43)$$

where I_1 denotes the moment of inertia of the left finger around the origin O and I_2 that of the right finger around O' . In this case, the sign of angles q_1 and θ is taken to be positive in the counter-clockwise direction but that of q_2 is taken to be positive in the clockwise direction.

Now, in light of the arguments developed in the previous two sections, it is rather evident that Lagrange's equation of motion of this fingers-object system is governed by the following set of equations:

$$I_i \ddot{q}_i - f_i \frac{\partial Q_i}{\partial q_i} - \lambda_i \frac{\partial R_i}{\partial q_i} = u_i, \quad i = 1, 2, \quad (2.44)$$

$$M \begin{pmatrix} \ddot{x} \\ \ddot{y} \end{pmatrix} - \sum_{i=1,2} \left\{ f_i \begin{pmatrix} \partial Q_i / \partial x \\ \partial Q_i / \partial y \end{pmatrix} + \lambda_i \begin{pmatrix} \partial R_i / \partial x \\ \partial R_i / \partial y \end{pmatrix} \right\} = 0, \quad (2.45)$$

$$I \ddot{\theta} - \sum_{i=1,2} \{ f_i (\partial Q_i / \partial \theta) + \lambda_i (\partial R_i / \partial \theta) \} = 0, \quad (2.46)$$

where

$$Q_i = -(l_i + r_i) - (-1)^i \{ (x - x_{0i}) \cos \theta - (y - y_{0i}) \sin \theta \} = 0, \quad i = 1, 2 \quad (2.47)$$

$$\frac{d}{dt} r_i \phi_i = -\frac{dY_i}{dt}, \quad i = 1, 2 \quad (2.48)$$

$$\begin{cases} Y_i = (x_{0i} - x) \sin \theta + (y_{0i} - y) \cos \theta \\ \phi_i = \pi - (-1)^i \theta - q_i \end{cases} \quad i = 1, 2 \quad (2.49)$$

$$\begin{aligned} R_i &= Y_i + r_i (\phi_i - \pi) - c_{0i} \\ &= (x_{0i} - x) \sin \theta + (y_{0i} - y) \cos \theta - c_{0i} - r_i \{ (-1)^i \theta + q_i \} \\ &= 0, \end{aligned} \quad i = 1, 2 \quad (2.50)$$

and c_{0i} denotes an appropriate constant. Equation (2.47) for i signifies the contact constraint at the contact point O_{0i} and Equation (2.48) for i captures the rolling constraint at the same point O_{0i} . Since Equation (2.48) can be

Table 2.1. Partial differentials of Q_i and R_i

$$\begin{array}{l}
 \left\{ \begin{array}{l} \frac{\partial Q_i}{\partial q_i} = (-1)^i J_{0i}^T(q_i) \begin{pmatrix} \cos \theta \\ -\sin \theta \end{pmatrix} \\ \frac{\partial R_i}{\partial q_i} = J_{0i}^T(q_i) \begin{pmatrix} \sin \theta \\ \cos \theta \end{pmatrix} - r_i \end{array} \right. \quad i = 1, 2 \\
 \\
 \left\{ \begin{array}{l} \frac{\partial Q_i}{\partial x} = (-1)^i \cos \theta, \quad \frac{\partial Q_i}{\partial y} = (-1)^i \sin \theta \\ \frac{\partial R_i}{\partial x} = -\sin \theta, \quad \frac{\partial R_i}{\partial y} = -\cos \theta \end{array} \right. \quad i = 1, 2 \\
 \\
 \left\{ \begin{array}{l} \frac{\partial Q_i}{\partial \theta} = -(-1)^i Y_i \\ \frac{\partial R_i}{\partial \theta} = (-1)^i l_i \end{array} \right. \quad i = 1, 2 \\
 \\
 J_{0i}^T(q_i) = \frac{\partial(x_{0i}, y_{0i})}{\partial q_i} = l_i \left((-1)^i \sin q_i, \cos q_i \right), \quad i = 1, 2 \\
 \text{where } l_1 = \text{the length of } \overline{OO_{01}} \\
 \text{and } l_2 = \text{that of } \overline{O'O_{02}}
 \end{array}$$

integrated and Y_i and ϕ_i can be expressed as in Equation (2.49), the rolling constraint can be rewritten in the form of the holonomic constraint shown in Equation (2.50). Therefore, the Lagrangian L of the overall system can be expressed as

$$L = K + \sum_{i=1,2} \{f_i Q_i + \lambda_i R_i\} \quad (2.51)$$

and thereby Equations (2.44) to (2.46) follow from applying the variational principle for the Lagrangian L . For the sake of convenience, we have calculated all partial differentials of Q_i and R_i in q_i , x , y and θ , which are given in Table 2.1. Substituting all these partial differentials into Equations (2.44) to (2.46) leads to

$$I_i \ddot{q}_i - f_i (-1)^i J_{0i}^T(q_i) \begin{pmatrix} \cos \theta \\ -\sin \theta \end{pmatrix} - \lambda_i \left\{ J_{0i}^T(q_i) \begin{pmatrix} \sin \theta \\ \cos \theta \end{pmatrix} - r_i \right\} = u_i, \quad i = 1, 2 \quad (2.52)$$

$$M \begin{pmatrix} \ddot{x} \\ \ddot{y} \end{pmatrix} - (f_1 - f_2) \begin{pmatrix} \cos \theta \\ -\sin \theta \end{pmatrix} + (\lambda_1 + \lambda_2) \begin{pmatrix} \sin \theta \\ \cos \theta \end{pmatrix} = 0, \quad (2.53)$$

$$I\ddot{\theta} - f_1 Y_1 + f_2 Y_2 + l_1 \lambda_1 - l_2 \lambda_2 = 0. \quad (2.54)$$

Since it follows from the meaning of the constraints expressed by Equations (2.47) and (2.50) that

$$\begin{cases} \frac{dQ_i}{dt} = \dot{q}_i \frac{\partial Q_i}{\partial q_i} + \dot{x} \frac{\partial Q_i}{\partial x} + \dot{y} \frac{\partial Q_i}{\partial y} + \dot{\theta} \frac{\partial Q_i}{\partial \theta} \\ \frac{dR_i}{dt} = \dot{q}_i \frac{\partial R_i}{\partial q_i} + \dot{x} \frac{\partial R_i}{\partial x} + \dot{y} \frac{\partial R_i}{\partial y} + \dot{\theta} \frac{\partial R_i}{\partial \theta} \end{cases} \quad i = 1, 2 \quad (2.55)$$

the sum of multiplications of Equation (2.52) by \dot{q}_i ($i = 1, 2$) and Equation (2.54) by $\dot{\theta}$ and inner product between Equation (2.53) and $(\dot{x}, \dot{y})^T$ yields

$$\frac{d}{dt}K = \sum_{i=1,2} \dot{q}_i u_i. \quad (2.56)$$

Now, we are ready to discuss how to design a controller that can stabilise both translational and rotational motions of the object by balancing forces and torques affecting the object. Obviously from Equations (2.53) and (2.54), the wrench vectors exerted on the object are described as follows:

$$\begin{aligned} \mathbf{w}_{f1} &= f_1 \begin{pmatrix} -\cos \theta \\ \sin \theta \\ -Y_1 \end{pmatrix}, & \mathbf{w}_{f2} &= f_2 \begin{pmatrix} \cos \theta \\ -\sin \theta \\ Y_2 \end{pmatrix}, \\ \mathbf{w}_{\lambda 1} &= \lambda_1 \begin{pmatrix} \sin \theta \\ \cos \theta \\ l_1 \end{pmatrix}, & \mathbf{w}_{\lambda 2} &= \lambda_2 \begin{pmatrix} \sin \theta \\ \cos \theta \\ -l_2 \end{pmatrix}. \end{aligned} \quad (2.57)$$

In order that the sum of these four wrenches become zero, it is necessary and sufficient that

$$f_1 = f_2 = f_d, \quad \lambda_1 + \lambda_2 = 0, \quad -f_d(Y_1 - Y_2) + \lambda_1(l_1 + l_2) = 0, \quad (2.58)$$

where f_d must be some positive constant. One possible solution to the simultaneous conditions of Equation (2.58) is to control the overall system motion so as to let $f_i \rightarrow f_d$, $Y_1 - Y_2 \rightarrow 0$ and $\lambda_i \rightarrow 0$ ($i = 1, 2$). Following this observation, we are able to devise the following control signal:

$$u_i = -c_i \dot{q}_i - (-1)^i f_d \left\{ J_{0i}^T(q_i) \begin{pmatrix} \cos \theta \\ -\sin \theta \end{pmatrix} - \frac{r_i}{r_1 + r_2} (Y_1 - Y_2) \right\} \quad (2.59)$$

where f_0 can be chosen as being equal to f_d or any other positive constant. Substituting Equation (2.59) into Equation (2.52) yields

$$\begin{aligned} I_i \ddot{q}_i + c_i \dot{q}_i - (-1)^i \left\{ \Delta f_i J_{0i}^T(q_i) \begin{pmatrix} \cos \theta \\ -\sin \theta \end{pmatrix} + \frac{r_i f_d}{r_1 + r_2} (Y_1 - Y_2) \right\} \\ - \lambda_i \left\{ J_{0i}^T(q_i) \begin{pmatrix} \sin \theta \\ \cos \theta \end{pmatrix} - r_i \right\} = 0, \end{aligned} \quad (2.60)$$

where $\Delta f_i = f_i - f_0$ ($i = 1, 2$). We conveniently rewrite Equations (2.53) and (2.54) in the following equivalent formulae:

$$M \begin{pmatrix} \ddot{x} \\ \ddot{y} \end{pmatrix} - (\Delta f_1 - \Delta f_2) \begin{pmatrix} \cos \theta \\ -\sin \theta \end{pmatrix} + (\lambda_1 + \lambda_2) \begin{pmatrix} \sin \theta \\ \cos \theta \end{pmatrix} = 0, \quad (2.61)$$

$$I\ddot{\theta} - \Delta f_1 Y_1 + \Delta f_2 Y_2 - f_d(Y_1 - Y_2) + l_1 \lambda_1 - l_2 \lambda_2 = 0. \quad (2.62)$$

Similarly to the derivation of Equation (2.56) by referring to Equation (2.55), the sum of the multiplications of Equation (2.60) by \dot{q}_i for $i = 1, 2$, Equation (2.62) by $\dot{\theta}$, and the inner product between Equation (2.61) and $(\dot{x}, \dot{y})^T$ takes the form

$$\frac{d}{dt}K + \sum_{i=1,2} \left\{ c_i \dot{q}_i^2 - (-1)^i \frac{r_i f_d}{r_1 + r_2} \dot{q}_i (Y_1 - Y_2) \right\} - f_d \dot{\theta} (Y_1 - Y_2) = 0. \quad (2.63)$$

Since from Equations (2.48) and (2.49) it follows that

$$\begin{aligned} \dot{Y}_1 - \dot{Y}_2 &= -r_1 \dot{\phi}_1 + r_2 \dot{\phi}_2 = -r_1(\dot{\theta} - \dot{q}_1) + r_2(-\dot{\theta} - \dot{q}_2) \\ &= -(r_1 + r_2)\dot{\theta} + (r_1 \dot{q}_1 - r_2 \dot{q}_2) \end{aligned} \quad (2.64)$$

Equation (2.63) can be reduced to

$$\frac{d}{dt}E(\mathbf{X}, \dot{\mathbf{X}}) = - \sum_{i=1,2} c_i \dot{q}_i^2, \quad (2.65)$$

where $\mathbf{X} = (q_1, q_2, x, y, \theta)^T$,

$$P = \frac{f_d}{2(r_1 + r_2)}(Y_1 - Y_2)^2, \quad (2.66)$$

$$\begin{aligned} E(\mathbf{X}, \dot{\mathbf{X}}) &= K + P \\ &= \sum_{i=1,2} \frac{I_i}{2} \dot{q}_i^2 + \frac{M}{2}(\dot{x}^2 + \dot{y}^2) + \frac{I}{2} \dot{\theta}^2 + \frac{f_d}{2(r_1 + r_2)}(Y_1 - Y_2)^2, \end{aligned} \quad (2.67)$$

and K is the total kinetic energy already given by Equation (2.43). Equation (2.65) can be interpreted as stating that the time rate of the total energy $E(\mathbf{X})$ is equal to the instantaneous energy dissipation rate. Hence, we call the scalar function P the artificial potential. It is important to note that the closed-loop dynamics of Equations (2.60–2.62) is equivalent to Lagrange's equation of motion for the Lagrangian

$$L = K - P + \sum_{i=1,2} \{ \Delta f_i Q_i + \lambda_i R_i \}. \quad (2.68)$$

Note that the overall fingers–object system of Figure 2.9 has a single DOF because the system has five independent position variables $\mathbf{X} = (q_1, q_2, x, y, \theta)^T$ but they are subject to four independent holonomic constraints. Therefore P is positive definite with respect to \mathbf{X} under the four constraints and therefore the total energy $E(\mathbf{X}, \dot{\mathbf{X}})$ is positive definite for the state variables $(\mathbf{X}, \dot{\mathbf{X}})$ under the following eight constraints

$$\begin{cases} Q_i = 0, & R_i = 0 \\ \dot{Q}_i = \dot{\mathbf{X}}^T \frac{\partial Q_i}{\partial \mathbf{X}} = 0, & \dot{R}_i = \dot{\mathbf{X}}^T \frac{\partial R_i}{\partial \mathbf{X}} = 0 \end{cases} \quad i = 1, 2. \quad (2.69)$$

Hence, due to Dirichlet's theorem of stability, the equilibrium state $(\mathbf{X}_\infty, \dot{\mathbf{X}}_\infty = 0)$ that satisfies $Y_1 - Y_2 = 0$ at $\mathbf{X} = \mathbf{X}_\infty$ is stable.

Now, we show that the equilibrium state $(\mathbf{X}_\infty, 0)$ is asymptotically stable for the system of Equations (2.60–2.62), *i.e.*, there exists a positive number $\delta > 0$ such that any solution $(\mathbf{X}(t), \dot{\mathbf{X}}(t))$ of Equations (2.60–2.62) subject to constraints (2.69) starting from an arbitrary initial state $(\mathbf{X}(0), \dot{\mathbf{X}}(0))$ satisfying $E(\mathbf{X}(0), \dot{\mathbf{X}}(0)) \leq \delta$ converges asymptotically to the equilibrium state $(\mathbf{X}_\infty, 0)$ as $t \rightarrow \infty$. For the sake of convenience for proving this, we rewrite the closed-loop dynamics of Equations (2.60–2.62) into the single matrix–vector form:

$$H\ddot{\mathbf{X}} + C\dot{\mathbf{X}} - A\Delta\boldsymbol{\lambda} - \frac{f_d}{r_1 + r_2}(Y_1 - Y_2)\mathbf{e} = 0 \quad (2.70)$$

where

$$H = \begin{pmatrix} I_1 & 0 & 0 & 0 & 0 \\ 0 & I_2 & 0 & 0 & 0 \\ 0 & 0 & M & 0 & 0 \\ 0 & 0 & 0 & M & 0 \\ 0 & 0 & 0 & 0 & I \end{pmatrix}, \quad \Delta\boldsymbol{\lambda} = \begin{pmatrix} \Delta f_1 \\ \Delta f_2 \\ \lambda_1 \\ \lambda_2 \end{pmatrix}, \quad \mathbf{e} = \begin{pmatrix} -r_1 \\ r_2 \\ 0 \\ 0 \\ r_1 + r_2 \end{pmatrix}, \quad (2.71)$$

$$A = \begin{pmatrix} -J_{01}^T \mathbf{r}_X & 0 & J_{01}^T \mathbf{r}_Y - r_1 & 0 \\ 0 & J_{02}^T \mathbf{r}_X & 0 & J_{02}^T \mathbf{r}_Y - r_2 \\ \mathbf{r}_X & -\mathbf{r}_X & -\mathbf{r}_Y & -\mathbf{r}_Y \\ Y_1 & -Y_2 & -l_1 & l_2 \end{pmatrix}, \quad (2.72)$$

$$C = \begin{pmatrix} c_1 & 0 & 0_{2 \times 3} \\ 0 & c_2 & 0_{3 \times 2} \\ 0_{3 \times 2} & 0_{3 \times 3} \end{pmatrix}, \quad \mathbf{r}_X = \begin{pmatrix} \cos \theta \\ -\sin \theta \end{pmatrix}, \quad \mathbf{r}_Y = \begin{pmatrix} \sin \theta \\ \cos \theta \end{pmatrix}. \quad (2.73)$$

Obviously, the 5×4 matrix A is of full rank [*i.e.*, $\text{rank}(A) = 4$] when the pair of fingers in contact with the object takes an ordinary position like that shown in Figure 2.9. The proof should go in the follows steps.

1) According to the energy relation of Equation (2.68), $E(\mathbf{X}(t), \dot{\mathbf{X}}(t)) \leq E(\mathbf{X}(0), \dot{\mathbf{X}}(0)) \leq \delta$ for any $t > 0$. Hence, $\dot{\mathbf{X}}(t)$ is uniformly bounded and $Y_1 - Y_2$ is also bounded, in particular

$$|Y_1(t) - Y_2(t)| \leq \sqrt{\frac{2(r_1 + r_2)\delta}{f_d}}. \quad (2.74)$$

2) Next, note that

$$\begin{aligned} 0 = \dot{R}_1 - \dot{R}_2 &= (\dot{x}_{01} - \dot{x}_{02}) \sin \theta + (\dot{y}_{01} - \dot{y}_{02}) \cos \theta \\ &\quad - \dot{\theta}(l_1 + l_2 + r_1 + r_2) + (r_1 + r_2)\dot{\theta} - r_1\dot{q}_1 - r_2\dot{q}_2 \end{aligned} \quad (2.75)$$

from which it follows that

$$\dot{\theta} = \frac{1}{l_1 + l_2} \{-r_1\dot{q}_1 + r_2\dot{q}_2 + (\dot{x}_{01} - \dot{x}_{02}) \sin \theta + (\dot{y}_{01} - \dot{y}_{02}) \cos \theta\}. \quad (2.76)$$

Hence, $|\dot{\theta}|$ is bounded. Similarly, it follows from differentiations of Q_1 and R_1 with respect to t that

$$R_\theta^T \begin{pmatrix} \dot{x} \\ \dot{y} \end{pmatrix} - R_\theta^T \begin{pmatrix} \dot{x}_{01} \\ \dot{y}_{01} \end{pmatrix} + \begin{pmatrix} Y_1\dot{\theta} \\ r_1\dot{q}_1 - l_1\dot{\theta} \end{pmatrix} = 0, \quad (2.77)$$

where

$$R_\theta = (\mathbf{r}_X \ \mathbf{r}_Y) = \begin{pmatrix} \cos \theta & \sin \theta \\ -\sin \theta & \cos \theta \end{pmatrix}. \quad (2.78)$$

Since R_θ is an orthogonal matrix, $R_\theta^{-1} = R_\theta^T$ and therefore Equation (2.77) is reduced to

$$\begin{pmatrix} \dot{x} \\ \dot{y} \end{pmatrix} = \begin{pmatrix} \dot{x}_{01} \\ \dot{y}_{01} \end{pmatrix} - R_\theta \begin{pmatrix} Y_1\dot{\theta} \\ r_1\dot{q}_1 - l_1\dot{\theta} \end{pmatrix} \quad (2.79)$$

from which $(\dot{x}, \dot{y})^T$ is also bounded.

3) Note that multiplication of Equation (2.70) from the left by $A^T H^{-1}$ yields

$$\begin{aligned} -\dot{A}^T \dot{\mathbf{X}} + A^T H^{-1} C \dot{\mathbf{X}} - A^T H^{-1} A \Delta \lambda \\ - \frac{f_d}{r_1 + r_2} (Y_1 - Y_2) A^T H^{-1} \mathbf{e} = 0, \end{aligned} \quad (2.80)$$

where we used the relation

$$0 = \frac{d}{dt}(A^T \dot{\mathbf{X}}) = A^T \ddot{\mathbf{X}} + \dot{A}^T \dot{\mathbf{X}}. \quad (2.81)$$

Multiplying Equation (2.80) by $(A^T H^{-1} A)^{-1}$ from the left yields

$$\Delta\lambda = (A^T H^{-1} A)^{-1} \left\{ -\dot{A}^T \dot{\mathbf{X}} + A^T H^{-1} C \dot{\mathbf{X}} - \frac{f_d}{r_1 + r_2} (Y_1 - Y_2) A^T H^{-1} \mathbf{e} \right\}. \quad (2.82)$$

Since A is of full rank at the equilibrium state $\mathbf{X} = \mathbf{X}_\infty$, it is possible to choose $\delta > 0$ small enough that A is nondegenerate for all \mathbf{X} satisfying $E(\mathbf{X}, \dot{\mathbf{X}}) \leq \delta$ together with constraints of Equation (2.69). Hence, $\Delta\lambda$ is also bounded.

4) Since $Y_1 - Y_2$, $\dot{\mathbf{X}}$, and $\Delta\lambda$ are all uniformly bounded, $\ddot{\mathbf{X}}$ must be uniformly bounded according to Equation (2.70). This implies that $\dot{\mathbf{X}}$ is uniformly continuous. In particular, \dot{q}_1 and \dot{q}_2 are uniformly continuous and also belong to $L^2(0, \infty)$ from the energy relation of Equation (2.65). Thus, on account of Lemma 2 of Appendix A, $\dot{q}_1(t)$ and $\dot{q}_2(t)$ converge to zero as $t \rightarrow \infty$. Then, according to Equations (2.76) and (2.79), $\dot{\theta}(t) \rightarrow 0$ as $t \rightarrow \infty$ and subsequently $\dot{x}(t)$ and $\dot{y}(t)$ must converge to zero as $t \rightarrow \infty$.

5) Since $\dot{\mathbf{X}}$ and $Y_1 - Y_2$ are uniformly continuous in t , $\ddot{\mathbf{X}}(t)$ is also uniformly continuous. Since $\dot{\mathbf{X}}$ is uniformly continuous and $\dot{\mathbf{X}}(t) \rightarrow 0$ as $t \rightarrow \infty$, Lemma A of Appendix A implies that $\ddot{\mathbf{X}}(t) \rightarrow 0$ as $t \rightarrow \infty$.

6) Thus, from Equation (2.70) it follows that

$$-[A, \mathbf{e}] \begin{bmatrix} \Delta\lambda \\ -f_d(Y_1 - Y_2)/(r_1 + r_2) \end{bmatrix} \rightarrow 0 \quad \text{as } t \rightarrow \infty. \quad (2.83)$$

Since the 5×5 -matrix $[A, \mathbf{e}]$ is nonsingular obviously, Equation (2.83) implies

$$Y_1(t) - Y_2(t) \rightarrow 0, \quad f_i(t) \rightarrow f_d, \quad \lambda_i(t) \rightarrow 0, \quad i = 1, 2 \quad (2.84)$$

as $t \rightarrow \infty$.

Thus, the proof of the asymptotic stability of the equilibrium state $(\mathbf{X}_\infty, 0)$ that satisfies $Y_1 - Y_2 = 0$ together with $f_i = f_d$ and $\lambda_i = 0$ has been completed.

However, there still remain uncertainties in the mathematical rigour of the proof and the practical effectiveness of the control scheme given by Equation (2.59). In fact, we could not argue how rapidly the solution trajectory $(\mathbf{X}(t), \dot{\mathbf{X}}(t))$ of Equation (2.70) converges to the equilibrium state $(\mathbf{X}_\infty, 0)$. We could not find out how large a neighbourhood of the equilibrium point $(\mathbf{X}_\infty, 0)$ characterised by $E(\mathbf{X}(0), \dot{\mathbf{X}}(0)) \leq \delta$ with $\delta > 0$ can be selected. If any solution trajectories starting from any initial state inside such a neighbourhood of $(\mathbf{X}_\infty, 0)$ converge asymptotically to $(\mathbf{X}_\infty, 0)$, the neighbourhood is called an attractor of the equilibrium point $(\mathbf{X}_\infty, 0)$. In the process of proving the asymptotic convergence, we needed to show that boundedness of the finger angular velocities \dot{q}_1 and \dot{q}_2 implies that of the velocities of the object variables (x, y, θ) based on Equations (2.76) and (2.79) owing to the four contact constraints. However, Equation (2.76) shows that the attractor of $(\mathbf{X}_\infty, 0)$ may not be selected large enough if the object width $l_1 + l_2$ is very small. Another problem is whether both contacts between the finger-ends and

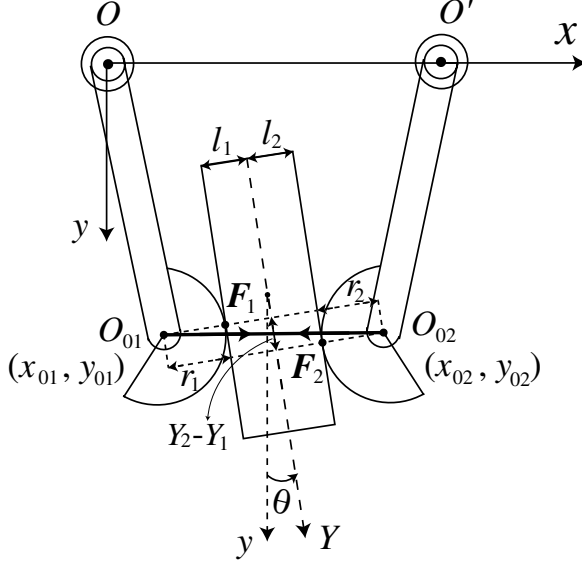


Fig. 2.10. A pair of single-DOF robot fingers grasping a 2-D object with parallel flat sides

object surfaces are maintained during the motion of the overall system. In the next section, a more mathematically rigorous treatment of the problem will be presented by introducing a far more important class of coordinated motor control signals for stable grasping.

2.6 Blind Grasping and Robustness Problems

Consider again a pair of dual single-DOF robot fingers contacting a 2-D rectangular object as shown in Figure 2.10. Now, let us consider the following class of control signals:

$$u_i = -c_i \dot{q}_i + (-1)^i \frac{f_d}{r_1 + r_2} J_{0i}^T(q_i) \begin{pmatrix} x_{01} - x_{02} \\ y_{01} - y_{02} \end{pmatrix}, \quad i = 1, 2. \quad (2.85)$$

The first term on the right-hand side indicates damping injection for finger joint motion and the second term is introduced to exert an approximated opposition force, denoted by \mathbf{F}_i in Figure 2.10, that presses the object coordinately from the left by the left finger ($i = 1$) and from the right by the right one ($i = 2$). If in the construction of the control signal of Equation (2.85) any information about the object is not available, *i.e.*, the positions of the contact points O_1 and O_2 are uncertain, we must use the information only about finger kinematics and measured data on finger joint angles. Hence we assume that

the Jacobian matrices $J_{0i}(q_i)$ for $i = 1, 2$ are known and the orientation vector $(x_{01} - x_{02}, y_{01} - y_{02})^T$ that has the same direction of $\overline{O_{01}O_{02}}$ is also known and available for the construction of the control signal. In other words, it is expected that the direction of the opposition force, coincident with the line $\overline{O_1O_2}$ but unknown, can be well approximated by the known axis of $\overline{O_{01}O_{02}}$.

Next, note that multiplication of Equation (2.85) by \dot{q}_i and summing the resultant equations for $i = 1, 2$ yields

$$\begin{aligned} & \sum_{i=1,2} \dot{q}_i u_i \\ &= - \sum_{i=1,2} c_i \dot{q}_i^2 - \frac{d}{dt} \left[\frac{f_d}{2(r_1 + r_2)} \{ (x_{01} - x_{02})^2 + (y_{01} - y_{02})^2 \} \right]. \end{aligned} \quad (2.86)$$

Then, it is easy to show (see Figure 2.10) that

$$(x_{01} - x_{02})^2 + (y_{01} - y_{02})^2 = (Y_1 - Y_2)^2 + l_w^2, \quad (2.87)$$

$$l_w = r_1 + r_2 + l_1 + l_2. \quad (2.88)$$

On the other hand, it follows from Equations (2.47) and (2.48) that

$$R_\theta^T \begin{pmatrix} x_{01} - x_{02} \\ y_{01} - y_{02} \end{pmatrix} = \begin{pmatrix} -l_w \\ Y_1 - Y_2 \end{pmatrix} \quad (2.89)$$

from which it follows that

$$\begin{pmatrix} x_{01} - x_{02} \\ y_{01} - y_{02} \end{pmatrix} = R_\theta \begin{pmatrix} -l_w \\ Y_1 - Y_2 \end{pmatrix} = -l_w \mathbf{r}_X + (Y_1 - Y_2) \mathbf{r}_Y. \quad (2.90)$$

Thus, the control signals u_i ($i = 1, 2$) can be recast into the form

$$\begin{aligned} u_i &= -c_i \dot{q}_i - (-1)^i f_0 J_{0i}^T(q_i) \mathbf{r}_X + \frac{f_d}{r_1 + r_2} (Y_1 - Y_2) (-1)^i \{ J_{0i}^T(q_i) \mathbf{r}_Y - \mathbf{r}_i \} \\ &\quad + (-1)^i \frac{r_i f_d}{r_1 + r_2} (Y_1 - Y_2), \end{aligned} \quad (2.91)$$

where

$$f_0 = \left(1 + \frac{l_1 + l_2}{r_1 + r_2} \right) f_d. \quad (2.92)$$

Substituting Equation (2.91) into Equation (2.52) yields

$$\begin{aligned} & I_i \ddot{q}_i - (-1)^i \Delta f_i J_{0i}^T(q_i) \mathbf{r}_X - \Delta \lambda_i \{ J_{0i}^T(q_i) \mathbf{r}_Y - \mathbf{r}_i \} \\ & \quad - (-1)^i \frac{r_i f_d}{r_1 + r_2} (Y_1 - Y_2) = 0, \quad i = 1, 2, \end{aligned} \quad (2.93)$$

where

$$\Delta f_i = f_i - f_0, \quad \Delta \lambda_i = \lambda_i + (-1)^i \frac{f_d}{r_1 + r_2} (Y_1 - Y_2), \quad i = 1, 2. \quad (2.94)$$

Note that Equation (2.93) becomes the same as Equation (2.60) if $\Delta \lambda_i$ is replaced with λ_i . Equations (2.53) and (2.54) can be rewritten as

$$M \begin{pmatrix} \ddot{x} \\ \ddot{y} \end{pmatrix} - (\Delta f_1 - \Delta f_2) \mathbf{r}_X + (\Delta \lambda_1 + \Delta \lambda_2) \mathbf{r}_Y = 0, \quad (2.95)$$

$$I \ddot{\theta} - \Delta f_1 Y_1 + \Delta f_2 Y_2 + \Delta \lambda_1 l_1 - \Delta \lambda_2 l_2 - f_d (Y_1 - Y_2) = 0. \quad (2.96)$$

These are also the same as Equation (2.61) and Equation (2.62), respectively, if $\Delta \lambda_i$ is replaced by λ_i for $i = 1, 2$. Thus, similarly to derivation of Equation (2.70), Equations (2.93), (2.95) and (2.96) can be recast in the vector-matrix equation:

$$H \ddot{\mathbf{X}} + C \dot{\mathbf{X}} - A \Delta \boldsymbol{\lambda} - \frac{f_d}{r_1 + r_2} (Y_1 - Y_2) \mathbf{e} = 0, \quad (2.97)$$

where

$$\Delta \boldsymbol{\lambda} = (\Delta f_1, \Delta f_2, \Delta \lambda_1, \Delta \lambda_2)^T. \quad (2.98)$$

Note that this $\Delta \boldsymbol{\lambda}$ differs slightly from that in Equation (2.71). Similarly, by taking inner product between Equation (2.97) and $\dot{\mathbf{X}}$ or substituting Equation (2.86) into Equation (2.56), we obtain

$$\frac{d}{dt} E(\mathbf{X}, \dot{\mathbf{X}}) = - \sum_{i=1,2} c_i \dot{q}_i^2, \quad (2.99)$$

where E is given by Equation (2.67). This relation is the same as Equation (2.65).

It can easily be reconfirmed that the closed-loop dynamics of Equations (2.93–2.96) is derived as Lagrange's equation of motion for the Lagrangian

$$L = K - P + \sum_{i=1,2} \{ \Delta f_i Q_i + \Delta \lambda_i R_i \}, \quad (2.100)$$

where Q_i and R_i ($i = 1, 2$) are defined by (2.47) and (2.50), K is given by (2.43) and P is the same artificial potential as given in (2.66). This means that the same argument developed in the previous section for proving the convergence of solution trajectories of Equation (2.70) can apply to Equations (2.93), (2.95) and (2.96) or Equation (2.97). Then, it is concluded that

$$Y_1(t) - Y_2(t) \rightarrow 0, \quad \Delta f_i(t) \rightarrow 0, \quad \Delta \lambda_i(t) \rightarrow 0, \quad i = 1, 2 \quad (2.101)$$

as $t \rightarrow \infty$. This means that

Table 2.2. Physical parameters

$m_{11} = m_{21}$	link mass	0.025[kg]
$I_{11} = I_{21}$	inertia moment	$3.333 \times 10^{-6}[\text{kg} \cdot \text{m}^2]$
$l_{11} = l_{21}$	link length	0.040[m]
$r_1 = r_2$	radius	0.01[m]
M	object mass	0.027[kg]
h	object height	0.025[m]
$w = (l_1 + l_2)$	object width	0.03[m]
I	object inertia moment	$3.431 \times 10^{-6}[\text{kg} \cdot \text{m}^2]$
$l_1 = l_2$	object length	0.015[m]

Table 2.3. Parameters of the control signals

f_d	internal force	1.0[N]
$c_1 = c_2$	damping coefficient	0.002[msN]
γ_f	CSM gain	1500.0
γ_λ	CSM gain	3000.0

$$f_i(t) \rightarrow f_0, \quad \lambda_i(t) \rightarrow 0, \quad i = 1, 2 \quad (2.102)$$

as $t \rightarrow \infty$. This concludes that solution trajectories of Equation (2.97) converge asymptotically to the equilibrium state.

In order to see how rapidly such solution trajectories converge to the equilibrium state, we will show results of numerical simulation conducted on the basis of physical models of robot fingers and a 2-D rectangular object with regular size and weight as shown in Table 2.2. In this simulation, Baumgarte's constraint stabilisation method (CSM) is employed by introducing a class of over-damped second-order differential equation with gains γ_f and γ_λ to approximate the holonomic constraints well. The details of the CSM method will be given in Section 4.5. By using the control gains given in Table 2.3 and starting from the initial state with $\dot{\mathbf{X}}(0) = 0$ given in Table 2.3, we can obtain a numerical solution to Equation (2.97). In Figure 2.11 we show the transient behaviours of the key physical variables involved in Equation (2.97). As can be seen from Figure 2.11, $Y_1 - Y_2$, f_i and λ_i ($i = 1, 2$) converge asymptotically to each expected constant value. As a matter of course, the rotational angle θ of the object also converges asymptotically to a certain constant. Furthermore, all the transient behaviours of the physical variables suggest that the speed of all these convergences must be exponential in t . In the next section, we shall confirm this exponential convergence of the solution trajectories in a rigorous mathematical way.

Before closing the section we will show another coordinated control signal for establishing force/torque balance for the physical setup shown in Figure 2.10. This is of the form

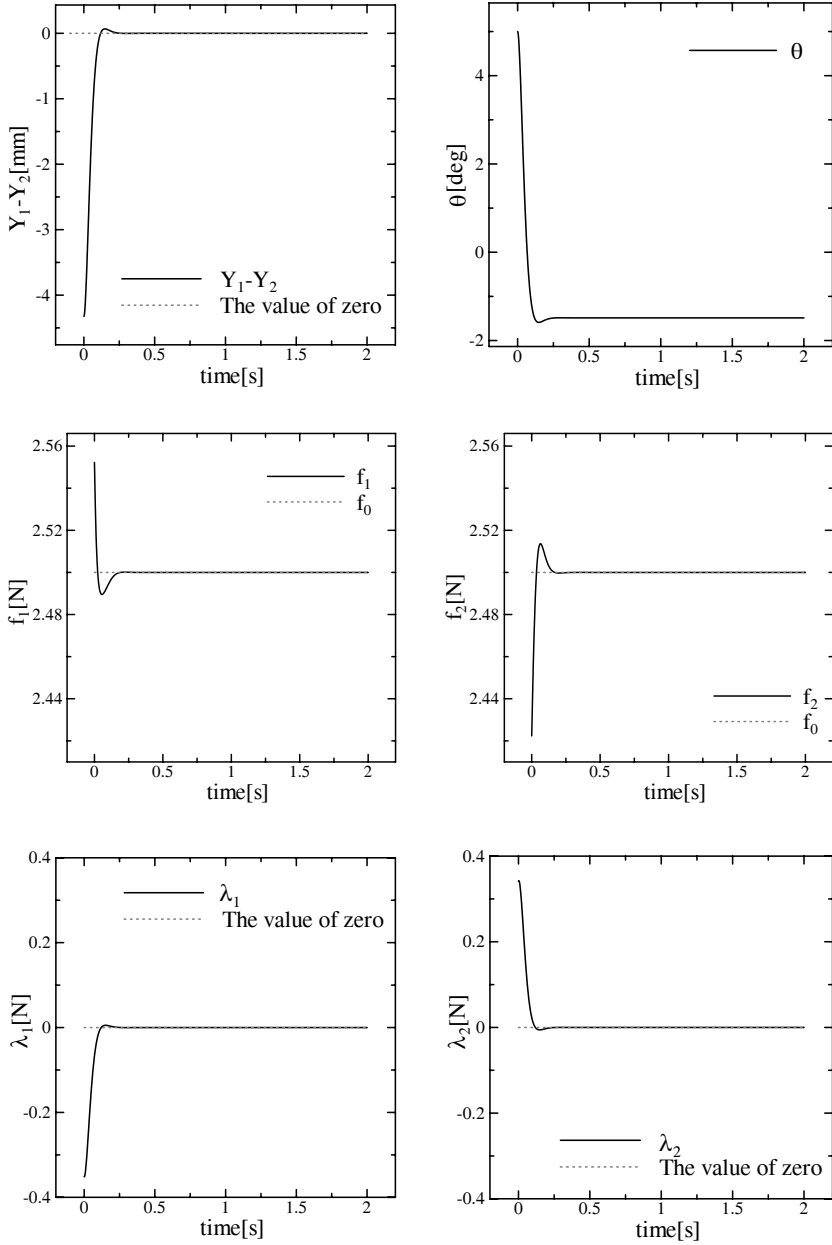


Fig. 2.11. The transient responses of physical variables along a solution to Equation (2.97) when the control signals of Equation (2.85) are exerted on finger joints

$$u_i = -c_i \dot{q}_i + (-1)^i \frac{f_d}{r_1 + r_2} J_{0i}^T(q_i) \begin{pmatrix} x_{01} - x_{02} \\ y_{01} - y_{02} \end{pmatrix} - r_i \hat{N}_i, \quad i = 1, 2 \quad (2.103)$$

where

$$\begin{aligned} \hat{N}_i(t) &= \hat{N}_i(0) + \gamma_i^{-1} \int_0^t r_i \dot{q}_i(\tau) d\tau \\ &= \hat{N}_i(0) + (r_i/\gamma_i) \{q_i(t) - q_i(0)\}, \quad i = 1, 2. \end{aligned} \quad (2.104)$$

The closed-loop dynamics obtained by substituting Equation (2.103) into Equation (2.52) can be written as the vector-matrix form

$$H \ddot{\mathbf{X}} + C \dot{\mathbf{X}} - A \Delta \boldsymbol{\lambda} - \frac{f_d}{r_1 + r_2} (Y_1 - Y_2) \mathbf{e} + \sum_{i=1,2} r_i \hat{N}_i \mathbf{e}_i = 0, \quad (2.105)$$

where

$$\mathbf{e}_1 = (1, 0, 0, 0, 0)^T, \quad \mathbf{e}_2 = (0, 1, 0, 0, 0)^T. \quad (2.106)$$

Then, it is easy to see that taking inner product between Equation (2.105) and $\dot{\mathbf{X}}$ yields

$$\frac{d}{dt} E_N(\mathbf{X}, \dot{\mathbf{X}}) = - \sum_{i=1,2} c_i \dot{q}_i^2, \quad (2.107)$$

where

$$E_N(\mathbf{X}, \dot{\mathbf{X}}) = K + P_N, \quad (2.108)$$

$$P_N = \frac{f_d}{2(r_1 + r_2)} (Y_1 - Y_2)^2 + \sum_{i=1,2} \frac{\gamma_i}{2} \hat{N}_i^2. \quad (2.109)$$

Applying a similar argument to that given in verifying the convergence of solution trajectories to Equation (2.97), we can conclude that $\dot{\mathbf{X}}$ and $\ddot{\mathbf{X}}$ tend to vanish as $t \rightarrow \infty$ and thereby as $t \rightarrow \infty$

$$A \Delta \boldsymbol{\lambda} + \frac{f_d}{r_1 + r_2} (Y_1 - Y_2) \mathbf{e} - \sum_{i=1,2} r_i \hat{N}_i \mathbf{e}_i \rightarrow 0. \quad (2.110)$$

Since matrix $[A, \mathbf{e}]$ is of 5×5 and non-singular at a regular position of the fingers-object setup shown in Figure 2.10, it is expected from Equation (2.110) that as $t \rightarrow \infty$ physical variables Δf_i , $\Delta \lambda_i$ ($i = 1, 2$), $Y_1 - Y_2$ and \hat{N}_i ($i = 1, 2$) may converge to some constant respectively. More explicitly, let us consider the minimisation problem:

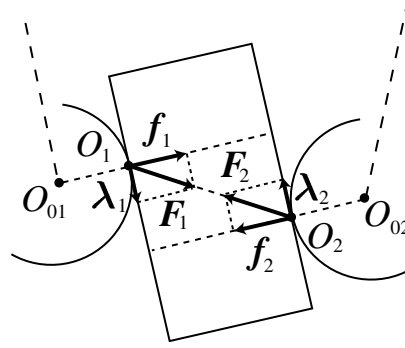


Fig. 2.12. Pressing forces \mathbf{F}_1 and \mathbf{F}_2 on the object must be collinear and oppositely directed

Table 2.4. Parameters of the control signals

f_d	internal force	1.0[N]
$c_1 = c_2 = c_m$	damping coefficient	0.002[msN]
$\gamma_i (i = 1, 2)$	regressor gain	0.001
$\hat{N}_i(0) (i = 1, 2)$	initial estimate value	0.0
γ_f	CSM gain	1500.0
γ_λ	CSM gain	3000.0

$$\left\{ \begin{array}{l} \text{Minimise } P_N = \frac{f_d}{2(r_1 + r_2)}(Y_1 - Y_2)^2 + \frac{\gamma_1}{2}\hat{N}_1^2 + \frac{\gamma_2}{2}\hat{N}_2^2 \\ \text{under the constraints} \\ Q_1 = 0, \quad Q_2 = 0, \quad R_1 = 0, \quad R_2 = 0 \end{array} \right.$$

Then, the solution $\mathbf{X} = \mathbf{X}^*$ that minimises P_N under the above constraints must satisfy the equations

$$A\Delta\lambda + \frac{f_d}{r_1 + r_2}(Y_1 - Y_2)\mathbf{e} = r_1\hat{N}_1\mathbf{e}_1 + r_2\hat{N}_2\mathbf{e}_2. \quad (2.111)$$

The minimising position state $\mathbf{X} = \mathbf{X}^*$ actually happens in a physical state as shown in Figure 2.12 where the pressing force \mathbf{F}_1 to the object from the left finger and \mathbf{F}_2 from the right finger must be collinear and oppositely directed. Before ascertaining this observation theoretically, we show how fast a solution to Equation (2.105) tends to the position $\mathbf{X} = \mathbf{X}^*$ that attains force/torque balance with the aid of computer simulation. Again, numerical simulation for the closed-loop dynamics of Equation (2.105) has been carried out by using the same physical parameters of the fingers-object system given in Table 2.2 and the control gains given in Table 2.4. We show the transient responses of the key physical variables in Figure 2.13. Apparently from the last two graphs

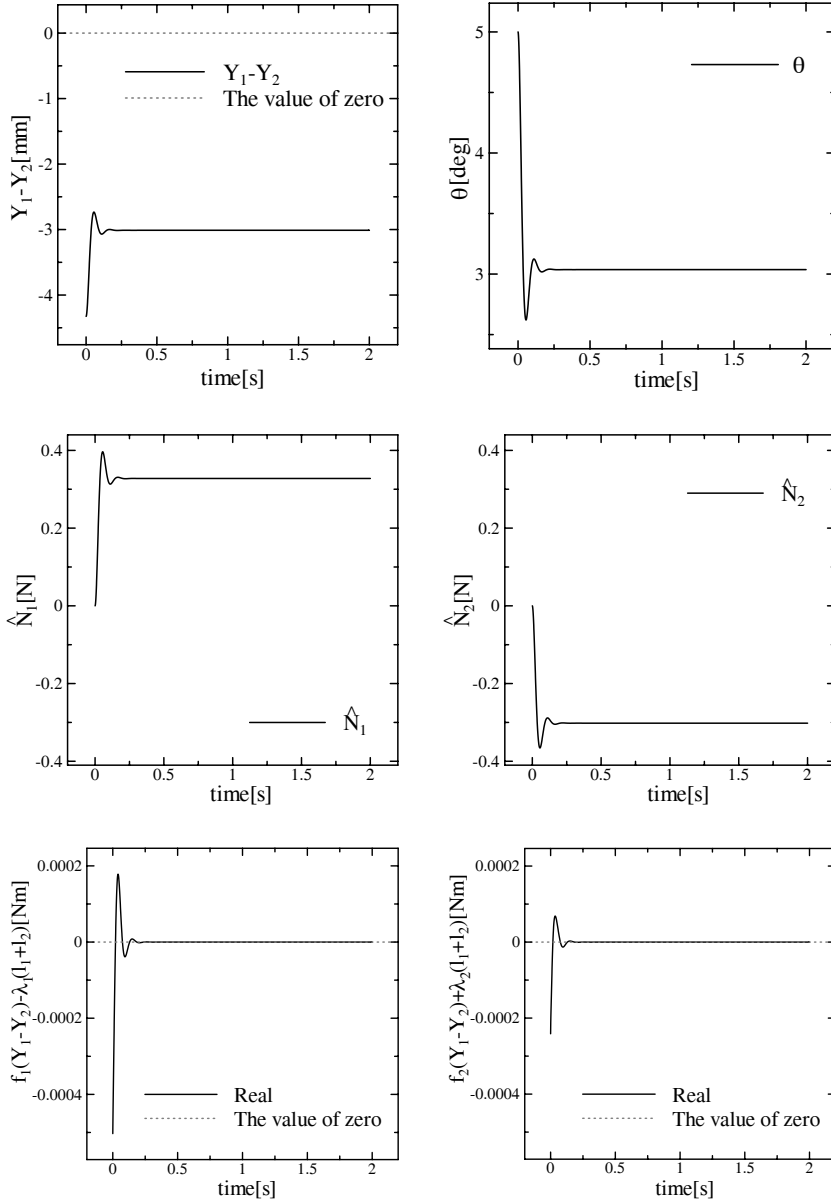


Fig. 2.13. The transient responses of physical variables along a solution to the closed-loop equation when the control signals of Equation (2.103) are used

of the figure, the solution converges to satisfy

$$f_i(Y_1 - Y_2) + (-1)^i \lambda_i(l_1 + l_2) = 0, \quad i = 1, 2, \quad (2.112)$$

which shows that as $t \rightarrow \infty$ force/torque balance is established.

Let us now find a solution satisfying Equation (2.111). Since x and y components of Equation (2.105) are the same as Equation (2.95), it should follow that

$$\Delta f_1 = \Delta f_2, \quad \Delta \lambda_1 = -\Delta \lambda_2. \quad (2.113)$$

Substituting this into Equation (2.96), we obtain

$$-\Delta f_1(Y_1 - Y_2) + \Delta \lambda_1(l_1 + l_2) - f_d(Y_1 - Y_2) = 0. \quad (2.114)$$

Subsequently, substituting Equation (2.94) into this equation yields

$$f_1(Y_1 - Y_2) + \lambda_1(l_1 + l_2) = 0, \quad (2.115)$$

which together with Equation (2.113) implies Equation (2.112). Thus, once f_1 is determined, the other magnitudes of the constraint forces f_2 , λ_1 , and λ_2 can be determined through Equations (2.113) and (2.115). The remaining six optimal values for the five components of \mathbf{X} and f_1 can be determined by six equations, which are 1) the first two components of Equation (2.105), where f_2 and λ_2 are substituted by f_1 and $-\lambda_1$, respectively, and again λ_1 is substituted by $-f_1(Y_1 - Y_2)/(l_1 + l_2)$ owing to Equation (2.115) and 2) the four constraint equations $Q_i = 0$ and $R_i = 0$ for $i = 1, 2$. Finally, we remark that the last term $-r_i \hat{N}_i$ of the control signal of Equation (2.103) plays a role of saving abundant joint movements from initial angles.

In view of these theoretical arguments and simulation results shown in Figure 2.13, $Y_1 - Y_2$ may not tend to zero as $t \rightarrow \infty$ and therefore the λ_i ($i = 1, 2$) also do not vanish with increasing t . This means that, around the state of force/torque balance of the fingers-object system (see Figure 2.9 or 2.10), the control torque inputs of Equation (2.103) generated at the finger joints are transmitted to the fingertips so as to withstand the reaction forces $-\mathbf{F}_i$ that are exerted on the contact points O_i for $i = 1, 2$. In other words, in this case non-zero tangential forces λ_i at the contact points to the object should be sustained by finger joint actuators even when the fingers-object state converges approximately to a still state attaining force/torque balance.

One of the advantages of using the coordinated control signal of Equation (2.103) is that it may be robust against the geometrical shapes of objects. In fact, the signals of Equation (2.103) can be constructed without knowing the geometrical shape of the object surface. In the next chapter, we shall discuss stability problems of the closed-loop dynamics when the same control signals as Equation (2.103) are used for 2-D objects with non-parallel but flat surfaces. Robustness problems of the control signals of Equation (2.103) for a general class of 2-D objects with smooth convex sides remain unsolved.

2.7 Exponential Convergence to Force/Torque Balance

Some of the arguments of the last two sections can be brought out more clearly and rigorously by discussing the speed of convergences of solution trajectories of the closed-loop dynamics toward the equilibrium point satisfying the balance of forces and torques acting on the object.

We consider the closed-loop Equation (2.97) of motion of the fingers-object system depicted in Figure 2.9 when the co-ordinated control signals of Equation (2.85) are used. First, we introduce a scale factor $r > 0$ and transform x and y to \bar{x} and \bar{y} in such a way that

$$\bar{x} = r^{-1}x, \quad \bar{y} = r^{-1}y. \quad (2.116)$$

Then, by defining $\bar{M} = r^2M$, we see that

$$\frac{1}{2}M(\dot{x}^2 + \dot{y}^2) = \frac{1}{2}\bar{M}(\dot{\bar{x}}^2 + \dot{\bar{y}}^2). \quad (2.117)$$

The reason why such a scale transformation is required is that Equation (2.61) expresses translational motion of the object on the basis of physical units [m] but Equations (2.60) and (2.62) express the rotational motion based on physical units [radian]. This was caused by the adoption of the generalized position coordinates $\mathbf{X} = (q_1, q_2, x, y, \theta)^T$ mixed with physical units [m] and [radian]. This also causes imbalance among the eigenvalues of the inertia matrix H defined in Equation (2.71). Therefore, once Equation (2.61) for the translational motion of the object is rewritten by this scale transformation as

$$\bar{M} \begin{pmatrix} \ddot{\bar{x}} \\ \ddot{\bar{y}} \end{pmatrix} - r(\Delta f_1 - \Delta f_2) \mathbf{r}_X + r(\lambda_1 + \lambda_2) \mathbf{r}_Y = 0 \quad (2.118)$$

Equation (2.70) can be written in the form

$$\bar{H} \ddot{\mathbf{X}} + C \dot{\mathbf{X}} - \bar{A} \Delta \boldsymbol{\lambda} - \frac{f_d}{r_1 + r_2} (Y_1 - Y_2) \mathbf{e} = 0, \quad (2.119)$$

where

$$\left\{ \begin{array}{l} \bar{\mathbf{X}} = (q_1, q_2, r^{-1}x, r^{-1}y, \theta), \quad \bar{\mathbf{r}}_X = r \begin{pmatrix} \cos \theta \\ -\sin \theta \end{pmatrix}, \\ \bar{H} = \begin{pmatrix} I_1 & 0 & 0 & 0 & 0 \\ 0 & I_2 & 0 & 0 & 0 \\ 0 & 0 & r^2M & 0 & 0 \\ 0 & 0 & 0 & r^2M & 0 \\ 0 & 0 & 0 & 0 & I \end{pmatrix}, \quad \bar{\mathbf{r}}_Y = r \begin{pmatrix} \sin \theta \\ \cos \theta \end{pmatrix}, \\ \bar{A} = \begin{pmatrix} -J_{01}^T \mathbf{r}_X & 0 & J_{01}^T \mathbf{r}_Y - r_1 & 0 \\ 0 & J_{02}^T \mathbf{r}_X & 0 & J_{02}^T \mathbf{r}_Y - r_2 \\ \bar{\mathbf{r}}_X & -\bar{\mathbf{r}}_X & -\bar{\mathbf{r}}_Y & -\bar{\mathbf{r}}_Y \\ Y_1 & -Y_2 & -l_1 & l_2 \end{pmatrix}. \end{array} \right. \quad (2.120)$$

It is also necessary to introduce the pseudo-inverse of 4×5 matrix \bar{A}^T , which is defined as

$$(\bar{A}^T)^+ = \bar{A} (\bar{A}^T \bar{A})^{-1}. \quad (2.121)$$

Evidently it follows that

$$\dot{\bar{X}}^T (\bar{A}^T)^+ = \dot{\bar{X}}^T \bar{A} (\bar{A}^T \bar{A})^{-1} = 0. \quad (2.122)$$

Let us define another important 5×5 matrix

$$P = I_5 - (\bar{A}^T)^+ \bar{A}^T = I_5 - \bar{A} (\bar{A}^T \bar{A})^{-1} \bar{A}^T. \quad (2.123)$$

Then, it is easy to see that

$$P \bar{A} = 0_{5 \times 4} \quad (2.124)$$

and it follows that

$$P^T = P, \quad PP = P, \quad e^T P e \leq e^T e \quad (2.125)$$

for any five-dimensional vector e .

Now we are in a position to prove the exponential convergence of a solution to Equation (2.119). First, note that taking inner product between Equation (2.119) and $Pe(Y_1 - Y_2)$ yields

$$e^T P \bar{H} \ddot{\bar{X}}(Y_1 - Y_2) + e^T P C \dot{\bar{X}}(Y_1 - Y_2) - \frac{f_d(Y_1 - Y_2)^2}{r_1 + r_2} e^T P e = 0 \quad (2.126)$$

from which it follows that

$$\begin{aligned} & \frac{d}{dt} \left\{ -e^T P \bar{H} \dot{\bar{X}}(Y_1 - Y_2) \right\} \\ &= -\frac{f_d(Y_1 - Y_2)^2}{r_1 + r_2} e^T P e + e^T P C \dot{\bar{X}}(Y_1 - Y_2) + h(\dot{\bar{X}}), \end{aligned} \quad (2.127)$$

where

$$h(\dot{\bar{X}}) = -e^T \left\{ \dot{P} \bar{H} \dot{\bar{X}}(Y_1 - Y_2) + P \bar{H} \dot{\bar{X}}(\dot{Y}_1 - \dot{Y}_2) \right\}. \quad (2.128)$$

Here, e signifies the five-dimensional vector defined in Equation (2.71). Since in general it follows that for any $\gamma > 0$

$$|ab| \leq \frac{1}{2} (\gamma a^2 + (1/\gamma) b^2) \quad (2.129)$$

we see that

$$e^T P C \dot{\bar{X}}(Y_1 - Y_2) \leq \frac{f_d(Y_1 - Y_2)^2}{2(r_1 + r_2)} e^T P e + \frac{r_1 + r_2}{2f_d} (c_1^2 \dot{q}_1^2 + c_2^2 \dot{q}_2^2). \quad (2.130)$$

Now we assume that at the equilibrium state $(\bar{\mathbf{X}}_\infty, 0)$ satisfying $Y_1 - Y_2 = 0$, $f_i = f_d$, $\lambda_i = 0$ ($i = 1, 2$) as discussed in the paragraph containing Equation (2.84) and its subsequent paragraphs, matrix \bar{A} is of full rank (non-degenerate) and the matrix $[\bar{A}, \mathbf{e}]$ is non-singular. Then, obviously at $\bar{\mathbf{X}} = \bar{\mathbf{X}}_\infty$, $\mathbf{e}^T P \mathbf{e}$ does not vanish. Let us define

$$0 < \gamma_e = \frac{\mathbf{e}^T P \mathbf{e}}{\mathbf{e}^T \mathbf{e}} = \left\{ 1 - \frac{\mathbf{e}^T (\bar{A}^T)^+ \bar{A}^T \mathbf{e}}{\mathbf{e}^T \mathbf{e}} \right\}, \quad (2.131)$$

which is evaluated at $\bar{\mathbf{X}} = \bar{\mathbf{X}}_\infty$. At this stage, we note that the Lyapunov function $E(\mathbf{X}, \dot{\mathbf{X}})$ [or equivalently, $E(\bar{\mathbf{X}}, \dot{\bar{\mathbf{X}}})$] is positive definite with respect to $(\bar{\mathbf{X}}, \dot{\bar{\mathbf{X}}})$ under the constraints $Q_i = 0$, $R_i = 0$, $\dot{Q}_i = 0$ and $\dot{R}_i = 0$ ($i = 1, 2$) in a neighbourhood of $\bar{\mathbf{X}} = \bar{\mathbf{X}}_\infty$. Hence, it is possible to choose $\delta > 0$ such that, at any $(\bar{\mathbf{X}}, \dot{\bar{\mathbf{X}}})$ satisfying

$$E(\bar{\mathbf{X}}, \dot{\bar{\mathbf{X}}}) = E(\mathbf{X}, \dot{\mathbf{X}}) < \delta \quad (2.132)$$

and constraints $Q_i = 0$ and $R_i = 0$ ($i = 1, 2$), $\mathbf{e}^T P \mathbf{e}$ also satisfies

$$\mathbf{e}^T P \mathbf{e} / \mathbf{e}^T \mathbf{e} \geq \frac{1}{2} \gamma_e \quad (2.133)$$

and in addition that the matrix \bar{A} is non-degenerate. Further, we choose f_d and c_i ($i = 1, 2$) so that they satisfy

$$\frac{(r_1 + r_2)c_i}{f_d \gamma_e \mathbf{e}^T \mathbf{e}} \leq \frac{1}{2} \quad i = 1, 2. \quad (2.134)$$

Then, by substituting inequality (2.130) into (2.127) and referring to Equations (2.133) and (2.134), we obtain

$$\begin{aligned} & \frac{d}{dt} \left\{ -\frac{2}{\gamma_e \mathbf{e}^T \mathbf{e}} \mathbf{e}^T P \bar{H} \dot{\bar{\mathbf{X}}} (Y_1 - Y_2) \right\} \\ & \leq -\frac{f_d (Y_1 - Y_2)^2}{2(r_1 + r_2)} + \frac{1}{2} (c_1 \dot{q}_1^2 + c_2 \dot{q}_2^2) + \frac{2}{\gamma_e \mathbf{e}^T \mathbf{e}} h(\dot{\bar{\mathbf{X}}}). \end{aligned} \quad (2.135)$$

Now, we define

$$V_\alpha = E(\bar{\mathbf{X}}, \dot{\bar{\mathbf{X}}}) - \frac{2\alpha}{\gamma_e \mathbf{e}^T \mathbf{e}} \mathbf{e}^T P \bar{H} \dot{\bar{\mathbf{X}}} (Y_1 - Y_2), \quad (2.136)$$

where α is a positive parameter such that $0 < \alpha \leq 1$. Obviously, V_α is a quadratic function of $\bar{\mathbf{X}}$, $\dot{\bar{\mathbf{X}}}$ and $Y_1 - Y_2$ and, according to Equations (2.99) and (2.135), the time derivative \dot{V}_α becomes

$$\begin{aligned} \frac{d}{dt} V_\alpha & \leq -\left(1 - \frac{\alpha}{2}\right) (c_1 \dot{q}_1^2 + c_2 \dot{q}_2^2) \\ & \quad - \frac{\alpha f_d}{2(r_1 + r_2)} (Y_1 - Y_2)^2 + \alpha \bar{h}(\dot{\bar{\mathbf{X}}}). \end{aligned} \quad (2.137)$$

where

$$\begin{aligned}\bar{h}(\dot{\mathbf{X}}) &= \frac{2}{\gamma_e \mathbf{e}^T \mathbf{e}} h(\dot{\mathbf{X}}) \\ &= -\frac{2}{\gamma_e \mathbf{e}^T \mathbf{e}} \mathbf{e}^T \left\{ \dot{P} \bar{H} \dot{\mathbf{X}} (Y_1 - Y_2) + P \bar{H} \dot{\mathbf{X}} (\dot{Y}_1 - \dot{Y}_2) \right\}. \quad (2.138)\end{aligned}$$

Note that this can be regarded as a quadratic function of $\dot{\mathbf{X}}$ and further $|Y_1 - Y_2|$ is at least of $O(r_1 + r_2)$. Hence, there is a constant β of $O(1)$ such that

$$\left| \bar{h}(\dot{\mathbf{X}}) \right| \leq \frac{\beta}{\gamma_e} K(\dot{\mathbf{X}}) = \frac{\beta}{\gamma_e} K(\dot{\mathbf{X}}), \quad (2.139)$$

where K denotes the kinetic energy defined by Equation (2.43). To simplify the mathematical argument, we assume at this stage that $c_1 = c_2 = c_{\max}$ and $r_1 = r_2 = r_m$. Furthermore, we assume that the object width $l_1 + l_2$ is not so small relative to r_i ($= r_m$). Then, as discussed around the derivation of Equations (2.76) and (2.79), it is possible to confirm that

$$\begin{cases} \dot{\theta}^2 \leq \beta_\theta (\dot{q}_1^2 + \dot{q}_2^2) \\ r^{-2} (\dot{x}^2 + \dot{y}^2) \leq \beta_0 (\dot{q}_1^2 + \dot{q}_2^2), \end{cases} \quad (2.140)$$

where β_θ and β_0 are positive constants of numerical order $O(1)$, and the scale factor r can be selected around $r = 0.01$ – 0.02 in relation to the physical parameters given in Tables 2.2 and 2.3. Then, the total kinetic energy must be of order

$$K(\dot{\mathbf{X}}) = \gamma (\dot{q}_1^2 + \dot{q}_2^2) \quad (2.141)$$

with a positive constant γ that is of $O(10^{-5})$. Thus, referring to Equations (2.139) and (2.141), we can conclude that

$$\begin{aligned} \frac{d}{dt} V_\alpha &\leq - \left(1 - \frac{\alpha}{2} - \frac{\alpha \beta \gamma}{\gamma_e c_m} \right) (c_m \dot{q}_1^2 + c_m \dot{q}_2^2) \\ &\quad - \frac{\alpha f_d}{2(r_1 + r_2)} (Y_1 - Y_2)^2. \end{aligned} \quad (2.142)$$

We now assume that γ_e defined by Equation (2.131) is large enough to satisfy $\gamma_e \geq 0.2$ and the finger joint damping coefficient c_m ($= c_1 = c_2$) is chosen around $c_m = 0.001$ – 0.003 [Nms]. Then, $\beta \gamma / \gamma_e c_m$ must be smaller than $1/4$ and therefore inequality (2.142) can be reduced to, in reference to Equation (2.141), the following fundamental inequality:

$$\frac{d}{dt} V_\alpha \leq -\alpha E(\bar{\mathbf{X}}, \dot{\mathbf{X}}). \quad (2.143)$$

Next, we evaluate the upper bound of scalar function V_α in the following way:

$$V_\alpha \leq E + \frac{\alpha}{\gamma_e \mathbf{e}^T \mathbf{e}} \left\{ \eta \mathbf{e}^T P \mathbf{e} (Y_1 - Y_2)^2 + \eta^{-1} \dot{\mathbf{X}}^T \bar{H} \bar{H} \dot{\mathbf{X}} \right\}. \quad (2.144)$$

Since $\mathbf{e}^T \mathbf{e} = (r_1 + r_2)^2 + r_1^2 + r_2^2 = 6r_m^2$ and $\mathbf{e}^T P \mathbf{e} / \mathbf{e}^T \mathbf{e} \leq 1$, choosing

$$\eta = \gamma_e f_d / 8(r_1 + r_2) = \gamma_e f_d / 16r_m \quad (2.145)$$

yields

$$V_\alpha \leq E + \frac{\alpha f_d}{8(r_1 + r_2)} (Y_1 - Y_2)^2 + \frac{8(r_1 + r_2)\alpha}{\gamma_e^2 f_d \mathbf{e}^T \mathbf{e}} \lambda_M(\bar{H}) K(\dot{\mathbf{X}}), \quad (2.146)$$

where $\lambda_M(\bar{H})$ denotes the maximum eigenvalue of \bar{H} . Since $\lambda_M(\bar{H})$ is of numerical order $O(10^{-6})$ and

$$\frac{8(r_1 + r_2)}{\gamma_e^2 f_d \mathbf{e}^T \mathbf{e}} = \frac{2 \times 10^2}{3r_m f_d} = O(10^4) \quad (2.147)$$

as far as f_d is of $O(1)$ in $[N]$, Equation (2.146) can be reduced to

$$V_\alpha \leq E + \frac{\alpha}{4} E = \left(1 + \frac{\alpha}{4}\right) E(\mathbf{X}, \dot{\mathbf{X}}). \quad (2.148)$$

From the same argument, it also follows that

$$V_\alpha \geq \left(1 - \frac{\alpha}{4}\right) E(\mathbf{X}, \dot{\mathbf{X}}), \quad (2.149)$$

that is,

$$\left(1 - \frac{\alpha}{4}\right) E \leq V_\alpha \leq \left(1 + \frac{\alpha}{4}\right) E \quad (2.150)$$

as far as $0 < \alpha \leq 1$. Thus, it follows from Equations (2.143) and (2.150) that

$$\frac{d}{dt} V_\alpha(t) \leq -\frac{4\alpha}{4 + \alpha} V_\alpha(t). \quad (2.151)$$

In particular, if we choose $\alpha = 1.0$, then it follows from Equations (2.150) and (2.151) that

$$E(\mathbf{X}(t), \dot{\mathbf{X}}(t)) \leq \frac{5}{3} E(\mathbf{X}(0), \dot{\mathbf{X}}(0)) e^{-0.8t}. \quad (2.152)$$

In conclusion, it has been proved that any solution $(\mathbf{X}(t), \dot{\mathbf{X}}(t))$ starting from an arbitrary initial state satisfying $E(\mathbf{X}(0), \dot{\mathbf{X}}(0)) < (3/5)\delta$ and constraints $Q_i = 0$, $R_i = 0$, $\dot{Q}_i = 0$ and $\dot{R}_i = 0$ for $i = 1, 2$ remains in the neighbourhood $M_1(\mathbf{X}_\infty) = \{(\mathbf{X}, \dot{\mathbf{X}}) : E(\mathbf{X}, \dot{\mathbf{X}}) < \delta \text{ and } Q_i = 0, R_i = 0, \dot{Q}_i = 0, \dot{R}_i = 0 \text{ for } i = 1, 2\}$ of $(\mathbf{X}_\infty, 0)$ and converges exponentially to the equilibrium point $(\mathbf{X}_\infty, 0)$.

The proof presented is based upon the numerical orders of the physical parameters of the fingers and object given in Table 2.2 and the control gains given in Table 2.3. That is, the proof is not generic but context dependent as is usually the case in human dexterity seen in our everyday life, as discussed in Section 1.4. Notwithstanding such context dependency, a similar mathematical argument can be developed for stability proof of grasping by similar fingers-object mechanisms with different numerical orders. However, it should be remarked that a synergistic choice for c_i (the damping factors for finger joints) and f_d satisfying Equation (2.134) is vital to regulate the exponential speed of convergence of solutions to the closed-loop dynamics. Furthermore, it should be noted that, if the object width $l_1 + l_2$ becomes small relative to the radius of the finger-end spheres, then the attractor region of convergence must be shrunk and the parameter α in the definition of the function V_α should be chosen considerably less than 1, that is, $0 < \alpha \ll 1.0$. Fortunately, however, human finger-ends are not rigid but rather soft and deformable. In Chapter 6 we will show that the visco-elastic properties of the finger-end material widen such attractor regions even if the object is very thin and light like a credit card or a paper name card.

Finally, the exponential convergence of solutions to the closed-loop dynamics in the case that the control signals of Equation (2.103) are used will be treated in Chapter 4 as a case of more general problems of grasping under the effect of gravity and the condition that the object has non-parallel flat surfaces.

Control Theory of Multi-fingered Hands
A Modelling and Analytical-Mechanics Approach for
Dexterity and Intelligence

Arimoto, S.

2008, IX, 271 p., Hardcover

ISBN: 978-1-84800-062-9